Report

Synthesis and Characterization of Biopolymers for Local Application against *Helicobacter pylori*

Vimon Tantishaiyakul
Krit Suknuntha
Nimit Warakul
Wirach Taweepreda
Wibul Wongpuwarak

Contents

Synthesis and Characterization of Biopolymers for Local Application against Helicobacter Pylori

Vimon Tantishaiyakul,[a] Krit Suknuntha,[a] Nimit Warakul,[b]
Wirach Taweepreda,[c] Wibul Wongpuwarak,[b]

[a]Department of Pharmaceutical Chemistry, [b]Department of Pharmaceutical Technology, Faculty of Pharmaceutical Sciences, [c]Polymer Science Program, Faculty of Science, Prince of Songkla University, Hat-Yai, Songkhla 90112 Thailand

Abstract

Mucoadhesion/bioadhesion of single polymer including chitosan (C), poly(vinyl pyrrolidone) (PVP), gelatin A (GA) and gelatin B (GB) , and blends were evaluated using texture analysis, viscometric method and HT29 cell attachment. These analyses demonstrate the higher mucoadhesion of some specific ratios of polymer blends than the single polymers. In addition, diffuse reflectance infrared Fourier transform spectroscopy (DRIFTS), ^{13}C cross-polarization magic angle-spinning nuclear magnetic resonance (^{13}C CP/MAS NMR) and molecular dynamic simulation were employed for evaluation of polymer-polymer as well as polymer-mucin (M) interactions. The results obtained shows that polymer-polymer and polymer-mucin can interact to each other and this may cause higher mucoadhesion/bioadheison. Metronidazole which is commonly drug use for treatment of *Helicobacter pylori* (*H. pylori*) infection is loaded in these polymer films. Drug released profiles show that mucoadhesive polymer can sustain drug release compared to that of drug alone.

1. Introduction

Mucoadhesive/bioadhesive polymers have received considerable attention for buccal retention or gastroretention of drugs.[1-5] Different molecular theories have been proposed to explain the mucoadhesion/bioadhesion phenomenon.[6] These include electronic theory, adsorption theory, wetting theory, diffusion theory and fracture theory.

Polymer blends have received a great deal of attention in recent years, since blending is a simple and effective method to develop new materials with specific properties that cannot be achieved by the individual polymer. Chitosan (C), (1-4)-2-amino-2-deoxy-β-D-glucan, is a natural polymer obtained by alkaline deacetylation of chitin, (1-4)-2-acetamido-2-deoxy-β-D-glucan. The molecule contains amino and hydroxyl groups on its backbone which can serve as proton donors/proton acceptors in hydrogen bonding interaction between chitosan molecules, or between chitosan and other polymers. Chitosan has been widely investigated for its potential use in industrial, medical and pharmaceutical applications. In addition to the use of chitosan as a single polymer, it is also often blended with various other hydrophilic polymers.[7-8] Chitosan/poly(vinyl pyrrolidone) (PVP) (both chemical structures shown in Figure 1), chitosan/gelatin A (GA) and chitosan/gelatin B (GB) blends have been prepared

and investigated for their potential use as controlled release drug delivery systems, and for enhancing mucoadhesive properties.[9, 10]

Generally, the chemical structures of the polymeric components have a significant effect on the interactions between the polymers. Various methods including viscosity measurement,[11-13] differential scanning calorimetry (DSC)[14] and Fourier transform infrared (FTIR) spectroscopy[11] have been previously used to explore the interactions between polymers. In addition, molecular modeling has been effectively used to study the interaction between two different species based on the calculation of radial distribution function (RDF).[15-17]

The objective of this study was to synthesize polymer blends and investigate the interactions of single polymers (C, PVP, GA and GB) with mucin; the interactions between polymer in blends (C-PVP, C-GA and C-GB); and these blends with mucin. These interactions were examined using diffuse reflectance infrared Fourier transform spectroscopy (DRIFTS), ^{13}C cross-polarization magic angle-spinning nuclear magnetic resonance (^{13}C CP/MAS NMR), molecular dynamic simulations, viscosity and texture analysis. In addition, bioadhesion analysis was performed using HT-29 cells. To investigate the potential uses of these polymers for *H. pylori* infection, metronidazole which is the commonly used drug for *H. pylori* infection was loaded in these polymers and blends. Drug release from these polymer films was also investigated.

2. Materials and methods

Chitosan, middle viscosity with a degree of deacetylation of 75-85%, was obtained from Fluka. PVP K-90 (Kollidon 90), with an average molecular weight ($\overline{M}_w$) of 1,100,000, was kindly supplied by BASF Thailand. Gelatin A and gelatin B were purchased from Sigma. Metronidazole was gifted by Siam Pharmaceutical, Thailand. Mucin type II from porcine stomach was obtained from Sigma (USA). All other reagents were of analytical grade.

2.1 Preparation of polymer blends

Stock solution (2% w/v) of each polymer was use for preparing polymer blend. Chitosan solution was prepared by dissolving 2 g of chitosan in 100 mL (0.05 M) HCl at ambient temperature with constant stirring overnight. Other polymers, PVP, GA and GB, were separately dissolved in water purified by reversed osmosis. The blends of C-PVP, C-GA and C-GB were prepared by mixing the stock solutions of specified polymers (2% w/v) in a 1:9, 3:7, 5:5, 7:3 and 9:1 volume ratio. For DRIFTS and texture analyses, 10 mL of these blends and each polymer solutions were poured into a polystyrene Petri dish and dried in an oven at 60 °C for 24 h. The films obtained were peeled off and kept in a desiccator under 50% RH until analyzed.

These blends and individual polymer were mixed with mucin solution for the study of the interaction between blends or single polymers with mucin as described in section 2.2.

2.2 Interaction of polymers/polymer blends and mucin

The stock solutions at 15% and 2% w/v of mucin were used for viscosity and DRIFTS studies, respectively. These stock solutions were mixed to each polymer blend in section 2.1 in 5 volume ratio using reciprocating shaker. The mixtures of polymer blends and mucin were directly used for viscosity measurement. For DRIFTS measurement, however, the mixtures were dried in the oven at 60°C for 24 h before analysis.

2.3 DRIFTS Spectra Collection

Polymer films were ground and placed in a micro sample cup for PerkinElmer Spectrum One FTIR diffuse reflectance accessory using the supplied sample cup holder. The FTIR measurements were performed on a PerkinElmer Spectrum One and a PerkinElmer DRIFTS accessory. The spectra were recorded from 4400 to 450 cm^{-1} by averaging 64 scans at 4 cm^{-1} resolution. All reflectance spectra were converted to Kubelka-Munk (KM) unit by the use of PerkinElmer Spectrum for Windows version 5.02 software package.

2.4 Viscosity

Viscosity measurements were performed using a Brookfield viscometer, model LVDV-III Ultra Programmable rheometer with a SC4-18 spindle and a small sample adaptor (Brookfield Engineering Laboratories, Inc., MA, USA), connected to a personal computer for setting analysis parameters and processing data. All measurements were carried out at 25°C after a rest time of 1 min. The apparent viscosity was measured at shear rates ranging from 3.96 to 79.2 s^{-1} (flow curve) after application of each shear rate for 1 min. Three measurements were performed for each sample.

The forces of mucoadhesion (F) between polymers or polymer blends with mucin involved physical chain entanglement, noncovalent intermolecular interactions can be calculated as described by Hassan and Gallo[18]

$$\eta_t = \eta_m + \eta_p + \eta_b$$
$$F = \eta_b \sigma$$

where η_t, η_m, and η_p are the viscosity coefficient of the system, mucin and the polymer, respectively, and σ is the rate of shear per second. These forces can be calculated if the viscosity of polymer solutions are Newtonian.

2.5 Texture Analysis

Polymer films were ground and prepared as discs (12 mm diameter) for texture analysis by direct compression using the Specac 15 ton manual hydraulic press (USA) and the discs were prepared using the Specac evacuable pellet die assembly. The discs were compressed at the pressure of 10 tons for 30 s and kept in desiccator until used.

Pig stomachs were obtained fresh from the slaughter house at Department of Natural Resources, Prince of Songkla University, Thailand. The stomachs were immediately washed with deionized water to remove non-digested food from lumen. This process was taken care to maintain the integrity of the mucus layer and the tissues were used within 6 hr.

The mucoadhesive strength of the polymer discs was investigated using the TA-XT2 texture analyzer (Stabel Micro Systems, Surrey, UK) with a 5 kg load cell equipped with mucoadhesive holder. The polymer disc was attached to the lower face of a horizontal cylindrical probe (diameter 14 mm) by double-sided adhesive tape.

The disc was moved to contact the soaked tissue and a downward force (0.1N) applied for 10 min. The probe was subsequently withdrawn at 1 mm s^{-1}. The mucoadhesion determined as the force of detachment could be detected directly from software Texture Expert version 1.22 which was used for data acquisition and analysis. The total amount of forces involved in the probe detachment (work of adhesion) was calculated from the area under the force of detachment vs distance curve.

2.6 Cell cultures

HT29 (passage 121-128) cells obtained from ATCC were grown, subcultured and maintained with Dulbecco's Modified Eagles Medium (DMEM) with 10% fetal calf serum (FCS), 1% non-essential amino acid and 1% L-glutamine at 5% CO_2, 95% O_2 at 37°C.

2.7 Bioadhesive studies

Polymer and polymer blend solutions (100 µL, 2% w/v) were casted on ultra low attachment surface microplates, 96-wells (Corning®), and dried in oven at 50°C. Acidity of chitosan solution causes cell death. Thus, all polymer films containing chitosan were neutralized by washing with 100 µl of 0.05M NaOH solution. These polymer coated plate was again dried in oven at 50°C. HT29 were seeded on this 96-wells plate at a density of 2×10^4 cell/cm^2. The cells were then incubated for 3 h in 5% CO_2, 95% O_2, 37°C. Subsequently, each well was washed twice with a sterile PBS solution to eliminate free cells. Then, a 3-(4,5-dimethylthiazol-2-yl)-2,5-diphenyl tetrazolium bromide (MTT) test was performed to quantify the viability of the cells which adhered on polymer films. The color developed was measured at 595 nm using Beckman Coulter DTX880 Multimode detectors with Multimode analysis software. This is compared to the control (without polymer).

2.8 Drug loading and release

Metronidazole solution (1% w/v) was prepared by dissolving 0.32 g of metronidazole in 32 mL of water and added to 20 mL polymer and polymer blend solution in section 2.1 to a final concentration of 0.2% w/v of metronidazole. The solution was mix using reciprocating shaker until homogeneous. Each polymer solution was then poured into a polystyrene Petri dish and dried in the oven at 60 °C for 24 h. The films obtained were peeled off and kept in a desiccator under 50% RH before drug release study.

The drug release rate from blended films was studied using the USP type II dissolution test apparatus (paddle). Drug release was performed using Vankel dissolution tester at 50 rpm. The drug loaded films were suspended in glass vessels containing 200 mL of medium which was maintained at 37 ± 0.5°C. The dissolution medium at pH 4 was prepared by dissolving 2.7218 g monobasic potassium phosphate (KH_2PO_4, MW=136.09) in 2000 mL H_2O and using either KOH or phosphoric acid to adjust the pH to 4. A 4.0 mL aliquot was withdrawn at appropriate time intervals and replaced with 4 mL of fresh dissolution medium. The amounts of metronidazole in dissolution media were determined using UV spectroscopy at 318 nm. The dissolution tests were performed in triplicate.

2.9 ^{13}C solid-state nuclear magnetic resonance (NMR) for PVP-chitosan blends

The NMR experiments were performed on a Bruker Avance 300 NMR spectrometer operating at 75.51 MHz for 13C using standard 4 mm cross-polarization magic angle-spinning probes (CP/MAS). The samples were spun at the magic angle at a rate of 10620 Hz with a total number scans of 10000. A ^{13}C contact time of 5.0 ms was used and a recycle delay between scans for all the samples was 3 s. The 13C chemical shifts were referenced with respect to tetramethylsilane (= 0 ppm) using solid adamantine as a secondary standard. There were no spinning side band (SSB) interferences as the samples were spun at 10 KHz. The deconvolution of NMR spectra was performed using GRAMS/AI7 by fitting the spectra with a Gaussian function.

2.10 Computational method for PVP-chitosan blends

Simulations of chitosan and PVP blend were performed using Materials Studio 4.2 (Accelrys, Inc.) on a dual core Pentium-based computer. A COMPASS (condensed-phase optimized molecular potentials for atomistic simulation studies) force field was employed for all calculations. This force field has been widely used to optimize and predict the conformation and thermophysical condensed phase properties of a broad range of molecules and polymers.[19]

Polymer assemblies containing 3 chains of PVP (20 monomer units) in its atatic stereochemical structure and 3 chains of chitosan (10 monomer units) were generated for the simulation of a 50:50 composition of the blend as previously conducted.[20] For the simulation of PVP:C 20:80, 33:67, 67:33 and 80:20 blends, 3 chains of each polymer were also employed but the numbers of monomer units were 20:40, 20:20, 40:10 and 80:10, respectively. Each generated polymer chain was minimized using the Discover module and the blend systems were built inside a box with periodic boundary conditions constructed using the amorphous cell module of the Materials Studio. The density of the blend system was estimated from densities of the pure polymers, i.e. 1.04 g/cm3 for PVP and 0.67 g/cm3 for C.[20] Thus, the simulation cell densities for PVP:C 20:80, 33:67, 50:50, 67:33 and 80:20 were 0.744, 0.792, 0.855, 0.917 and 0.966 g/cm3, respectively. The polymer assemblies were energy minimized using the steepest descent method followed by the conjugate gradient method with a convergence level of 0.01 kcal/mol/Å. Group-based cutoff of 12.5 Å and a switching function with the spline and buffer widths of 3 and 1 Å, respectively, were applied to evaluate nonbonded interactions. Molecular dynamics

simulations were performed in the NVT ensemble (constant particle numbers, volume and temperature) at 298 K with a time step of 1 fs. Molecular dynamics simulations were run for 1500 ps. Subsequently, the calculation of radial distribution function (RDF), g(r), was carried out of the trajectory files of simulations where the dynamic shows a stable performance.

3. Results and discussion

3.1 DRIFTS collection

DRIFTS spectra of C, mucin (M) and mixtures of C-M at volume ratios of 1:5, 3:5, 5:5, 7:5 and 9:5 are presented in Figure 2. Those of C, PVP and mixtures of C-PVP at volume ratios of 1:9, 3:7, 5:5 and 7:3 are shown in Figure 3. Figures 4-8 present the DRIFTS spectra of C-PVP 1:9 and C-PVP-M 1:9:5, C-PVP 3:7 and C-PVP-M 3:7:5, C-PVP 5:5 and C-PVP-M 5:5:5, C-PVP 7:3 and C-PVP-M 7:3:5, C-PVP 9:1 and C-PVP-M 9:1:5, respectively. DRIFTS of C, PVP and mucin also display in these figures for comparison. DRIFTS spectra of PVP, M and mixtures of PVP-M at volume ratios of 1:5, 3:5, 5:5, 7:5 and 9:5 are presented in Figure 9.

DRIFTS spectra of C, GA and blends of C:GA at volume ratios of 1:9, 3:7, 5:5 and 7:3 are shown in Figure 10. Figures 11-15 present the DRIFTS spectra of C-GA 1:9 and C-GA-M 1:9:5, C-GA 3:7 and C-GA-M 3:7:5, C-GA 5:5 and C-GA-M 5:5:5, C-GA 7:3 and C-GA-M 7:3:5, C-GA 9:1 and C-GA-M 9:1:5, respectively. DRIFTS of C, GA and M also show in these figures. DRIFTS spectra of GA, M and mixtures of GA-M at volume ratios of 1:5, 3:5, 5:5, 7:5 and 9:5 are presented in Figure 16.

DRIFTS spectra of C, GB and blends of C:GB at volume ratios of 1:9, 3:7, 5:5 and 7:3 are shown in Figure 17. Figures 18-22 present the DRIFTS spectra of C-GB 1:9 and C:GB:M 1:9:5, C-GB 3:7 and C:GB:M 3:7:5, C-GB 5:5 and C:GB:M 5:5:5, C-GB 7:3 and C:GB:M 7:3:5, C-GB 9:1 and C:GB:M 9:1:5, respectively. Those of C, GB and M also present in these figures. DRIFTS spectra of GB, M and mixtures of GB-M at volume ratios of 1:5, 3:5, 5:5, 7:5 and 9:5 are presented in Figure 23.

Due to board peaks at 3000-3700 cm^{-1}, it is difficult to observe the interaction between C-M, C-PVP or C-PVP-M. Details discussions of peak shift from chitosan were described in Section 3.3. These DRIFTS demonstrate the shift of characteristic peaks of each material (C, PVP, GA, GB and mucin) which in turn suggests the interaction between polymer-polymer, polymer-mucin and blends-mucin.

3.2 Viscosity measurement

In the preparation of samples for viscosity measurement, the stock solution concentration of polymers used is approximately 2% and that of mucin is about 15%. These solutions are mixed at the volume ratios as indicated in Table 1-3. Table 1 shows the force of mucoadhesion analysis by viscosity measurement for C-M, PVP-M and C-PVP blend-M. Force of mucoadhesion is highest in C-PVP blend at volume ratio of 1:1 (4.35 dyne/cm^2) followed by those of 0.6:1.4 (3.98 dyne/cm^2) and 0.2:1.8 (2.54 dyne/cm^2), respectively. These blends demonstrate higher mucoadhesive force than chitosan (2.31 dyne/cm^2) and PVP alone (1.23 dyne/cm^2).

Table 2 presents the force of mucoadhesion analysis for C-M, GA-M and C-GA blend-M. The highest mucoadhesive force obtained for the C-GA blends was at the volume ratio of 1.8:0.2 (2.26 dyne/cm^2). All C-GA blends demonstrate lower mucoadhesive force than chitosan (2.58 dyne/cm^2) but higher than GA alone (0.17 dyne/cm^2).

Table 3 shows the force of mucoadhesion analysis by viscosity measurement for C-M, GB-M and C-GB blend-M. The C-GB blends at volume ratios of 1:1 and 0.6:1:4 demonstrate highest mucoadhesive force (3.49 and 3.79 dyne/cm^2, respectively) which is significantly higher than chitosan (2.46 dyne/cm^2). The other blends exhibit lower mucoadhesive force than chitosan but higher than GB alone (0.57 dyne/cm^2).

Although the amount of chitosan used in each measurement was not exactly the same as its stock solution was prepared at different time of studies, the mucoadhesive forces for single polymers may be in the order of C > PVP > GB > GA. The blends of C-PVP and C-GB at some ratios demonstrate synergism in the interaction with mucin.

3.3 ^{13}C solid-state nuclear magnetic resonance (NMR) for PVP-chitosan blends

The ^{13}C-NMR chemical shifts or line shapes of carbon resonance in the cross-polarization/magic angle spinning (CP/MAS) spectra can provide information about the chemical environment of the carbon nucleus; therefore, their changes can indicate the intermolecular interactions between the blend components. The ^{13}C NMR spectra of PVP, chitosan and the 50:50 PVP/chitosan blend are shown in Figure 24. According to these ^{13}C-NMR spectra, the chemical shift of the PVP carbonyl carbon is observed at 176.23 ppm. This carbonyl carbon peak of the blend appears almost in the same chemical shift. However, its shape is broader and asymmetric compared to that of the pure PVP. Chen et al[21] have resolved ^{13}C CP/MAS NMR spectra at the carbonyl region to identify the crystalline and amorphous fractions of materials. In the present study, the carbonyl carbon peak of PVP in the blend was resolved into two Gaussian peaks using a curve-fitting procedure. PVP is an amorphous material. According to X-ray diffraction result, the PVP-C blend is also amorphous (data not shown). Hence, these two resolved peaks will not specify whether the form of PVP present is amorphous or crystalline. Multipeak curve fitting of NMR spectra has been previously signified as the occurrence of different interactions or environments of a specific group.[22, 23] Thus, in this study, the downfield shift of one peak may possibly result from the intermolecular hydrogen bonding between the carbonyl group of PVP and the hydrogen atom of OH-C6, OH-C3 or NH-C2 group of chitosan. The other peak may be the unreacted carbonyl carbon. As shown in Figure 24, the chemical shift of C2 and C6 of chitosan appears at 57.65 ppm and that of carbon atom C3 displays at 71.69 ppm which correspond to the previous assignment.[24] The upfield shifts of 0.70 (from 57.65 to 56.95 ppm) and 0.39 ppm (from 71.69 to 71.30 ppm) were observed for C2, 6 and C3, respectively, of the blend. As previously observed, the upfield shift of a carbon atom is attributed to the formation of hydrogen bonds of a connected proton donor group.[25] In the present study, the upfield shifts may therefore result from the intermolecular bonding between the proton donors of the OH groups at C3 and/or C6 as well as the NH group at C2 with C=O of PVP.

In addition to ^{13}C-CP/MAS NMR, DRIFTS was employed to investigate the interactions between these two polymers. DRIFTS spectra of PVP, C and the 50:50 PVP-C blend are shown in Figures 3 and 25. DRIFTS of the blend in Figure 25 was obtained from lyophilized material instead of film (Figure 3), however both spectra are similar. The spectrum of pure chitosan shows an amino band at 1637 cm^{-1}. In addition, chitosan displays a broad peak at around 3400 cm^{-1} resulting from the N-H and O-H vibrations. The amide carbonyl stretching of PVP shows a prominent peak at 1685 cm^{-1}. In the blend, this peak is shifted to the lower wavenumber at 1669 cm^{-1} indicating the incidence of interaction between PVP and chitosan. This interaction is attributed to the hydrogen bonds formed between the proton acceptor C=O of the PVP and the proton donor groups, such as OH-C6, OH-C3 and NH-C2 groups, of chitosan. Due to the overlapping band of OH and NH functions of chitosan, it is somewhat difficult to indicate which group is the proton donor in this system.

3.4 Computational method for PVP-chitosan blends

Molecular dynamics simulations and subsequent RDF calculations were performed to investigate the specific proton donor group of chitosan that interacts with the proton acceptor group of PVP. The RDF, also referred to as pair-correlation function, demonstrates the average density of atoms at a distance from a specified atom. The RDF analyses were performed in the interval of simulations where the simulation shows a stable behavior, i.e. from 800 to 1500 ps as illustrated in Figure 26. Figure 27 displays the intermolecular RDFs for the 50:50 PVP-C blend. As shown in Figure 27a, a pronounced peak at 1.75 Å with the g(r) function of 4.76 corresponds to the hydrogen bonding between the hydrogen atoms of OH-C6 of chitosan and the oxygen atoms of C=O of PVP. Meanwhile the g(r) function of about 2.81 at 1.75 Å was observed for hydrogen atoms of OH-C3 chitosan and oxygen atoms of C=O of PVP. This indicates that hydrogen atoms of OH-C6 form stronger hydrogen bonds with C=O of PVP than hydrogen atoms of OH-C3. This is possible due to the free rotation of OH-C6 compared to OH-C3 and consequently there is more accessibility to interact with oxygen atoms of PVP. This computational model is the first study that distinguishes the proton donor capacity between OH-C6 and OH-C3 of chitosan on interacting with other polymers.

The shift of the peak to 2.25 Å with the lower g(r) of 1.41 is related to the hydrogen atoms of NH-C2 of chitosan and the oxygen atoms of C=O of PVP. Therefore, the intermolecular hydrogen bond involving the amino group as the proton donor is significantly weaker than that of the hydroxyl groups of chitosan. This may be due to the fact that an N-H bond is less polar than an O-H bond. Thus the N-H···O=C hydrogen bond is weaker than the O-H···O=C counterpart. Figure 27b displays the RDF calculations for the nitrogen atom of PVP and the proton donors groups of chitosan. It can be observed that the amide nitrogen of PVP is less likely to function as a proton acceptor. Generally, nonbonding electron pairs of the amide nitrogen will delocalize to the carbonyl group. Therefore, in this case, when the proton donors of chitosan interact with the amide function of PVP, they will form a bond at the oxygen atom in preference to the nitrogen atom.

As proton acceptors, the oxygen atoms of the hydroxymethyl groups were previously reported to be more reactive than the nitrogen atoms of the amino groups of chitosan in forming hydrogen bonds with proton donors of polyvinyl alcohol

(PVA) or poly(2-hydroxyethyl methacrylate) (P2HEM) at some ratios of these polymer blends.[15, 26] However, with the higher amounts of PVA and P2HEM, the interactions with the amino groups of chitosan increase in intensity. Although, in the present study, proton donors and acceptors are reversed compared to the above-mentioned investigations, it was of interest to determine the interacting groups at different compositions of our polymer blend. Therefore, molecular dynamic simulations of PVP-C at compositions of 20:80, 33:67, 67:33 and 80:20 were performed and the RDFs for these blends were presented in Figures 28 and 29. The same results were obtained as the above-mentioned RDF for the 50:50 PVP-C blend, at either lower or higher amounts of PVP, hydrogen atoms of NH-C2 of chitosan function less as proton donors compared to those of OH-C6 and OH-C3. In the previous study, it was also observed that the interactions between hydrogen atoms of NH-C2 of chitosan and proton acceptor groups of P2HEM at various compositions of these blends were lower than those of the OH groups.[15]

Additionally, at lower amounts of PVP, the g(r) functions observed for the oxygen atom of C=O of PVP and the hydrogen atoms of OH-C6 and OH-C3 of chitosan are 6.29 and 2.52, respectively, for the 33:67 PVP-C blend (Figure 28a), and those of 5.76 and 1.70, respectively, for the 20:80 PVP-C blend (Figure 28b). Furthermore, for higher proportions of PVP, the g(r) functions for the oxygen atom of C=O of PVP and the hydrogen atoms of OH-C6 and OH-C3 of chitosan are 3.75 and 2.58, respectively, for the 67:33 PVP-C blend (Figure 29a) and those of 3.12 and 2.17, respectively, for the 80:20 PVP-C blend (Figure 29b). This indicates that the intermolecular hydrogen bonding between these two polymers is higher with lower amounts of PVP in the blends, and lower with the higher proportions of PVP (Figures 28 and 29, respectively). According to the previous investigations[10, 11] of various compositions of these two polymers blends, it demonstrates that these blends are miscible with only one glass transition temperature (Tg) was detected for each blend. In addition, the DSC thermograms of PVP-chitosan blends from both studies show positive deviations of Tgs from the linearity in the blends with lower PVP proportions whereas Tgs are lower in the blends with high amounts of PVP. Generally, the Tgs of polymer blends will be in the linear line which ranges between the initial Tg of each polymer depending on the relative amount of each polymer in the blend. However, if the two polymers bind more strongly to each other than to themselves, the Tg will be higher than expected (positive deviation from linearity). If the two polymers bind less strongly with each other than with themselves, the Tgs of the blends are lower than expected (negative deviation). Our dynamic simulations results are consistent with these findings[10, 11] in terms of positive/negative deviations related to the forces of intermolecular interactions between the polymers at lower/higher compositions of the PVP.

3.5 Texture analysis

Work of adhesion of chitosan, PVP, GA and GB blends were calculated from the area under the force of detachment vs distance curve as shown in Figure 30. Work of adhesion of chitosan, PVP and C-PVP blends are presented in Figure 31. The blend of C-PVP 5:5 demonstrates the highest work of adhesion which is higher than C or PVP alone. These results are consistent with those obtained using viscometric method.

Work of adhesion of C, GA and C-GA blends is shown in Figure 32. Work of adhesion of most C-GA blends is lower than that of chitosan. These results are consistent with those from viscometric method of C-GA blend.

Work of adhesion of C, GB and C-GB blends is shown in Figure 33. Work of adhesion of most C-GB blends is lower than chitosan. These results are slightly different from viscometric analysis.

A texture analysis is a convenient method for comparing work of adhesion among mucoadhesive polymers. This technique is used to support evidence of the interpenetration and hydrogen bonding between mucus and polymer. Due to different techniques use for mucoadhesive studies, the order of mucoadhesive force from texture analysis, C > GB > PVP > GA (Figures 31-33), is slightly different from that obtained from viscosity measurement C > PVP > GB > GA (Tables 1-3). However, both analyses demonstrate that some polymer blends of C-PVP and C-GB can enhance the mucoadhesive force than the single polymers.

3.6 Drug release

Dissolution profile of metronidazole alone, metronidazole loaded in single polymers and in various volume ratios of C-PVP, C-GA and C-GB blend films are shown in Figures 34-36, respectively.

Metronidazole is highly soluble in water (1g/100mL water)[27]. Its dissolution profile thus shows fast release of drug with the completely dissolving in 5 minutes. According to Figures 34-36, Metronidazole loaded in polymers and polymer blends is dissolved in about 20 minutes and drug releases from all single polymers or polymer blends are lower than drug alone. The dissolution profiles for the blends are comparable to those of single polymers, however, for some blends of C-GA and C-GB, the dissolution of the drug is lower than C, GA or GB. These results demonstrate that polymer blends can sustain drug release to some extent.

3.7 Bioadhesive study

HT29 monolayer is also used for cell adhesion study of polymers. This cell monolayer is suitable for bioadhesive investigation because of it can form monolayers of mature goblet cells under standard cell culture conditions. Besides, it can secrete mucin molecules and produce a mucus layer that covers the apical cell surface.[28]

Percent relative cell attachment of C-PVP, C-GA and C-GB blends using HT29 cell are shown in Figures 37, 38 and 39, respectively. These values for all single polymers are also presented along with their respective blends in these Figures. For single polymers, the order of cell attachment is PVP > C > GB > GA. Some C-PVP blends demonstrate higher bioadhesion than C or PVP alone. Most of C-GA and C-GB blends exhibit higher bioadhesion than C, GA or GB. These results show that cell adhesion of polymer blends at specific volume ratios are higher than those of single polymers. Probably due to different type of mucin from HT29 cells and procine stomach, the mucoadhesive/bioadhesive results obtained from texture analysis and viscosity measurement are different from those obtained using HT29 cells. However, according to studies based on these three techniques, C-PVP at 1:1 ratio

provides the highest mucoadhesive/bioadhesive force and most of C-GA and C-GB blends demonstrate higher mucoadhesive/bioadhesion than GA and GB.

In conclusion, DRIFTS, ^{13}C CP/MAS NMR and molecular modeling simulation demonstrate the presence of interactions between polymers and polymers-mucin. The intermolecular interactions between polymer-mucin can possibly enhance mucoadhesiv/bioadhesive force as examined using texture analysis, viscometric measurement and HT29 cell attachement. In this study, polymer blends of C-PVP, C-GA and C-GB at some ratios exhibit higher mocuadhesive/bioadhesive force than single polymers. In addition, these blends can sustain metronidazole release. The use of polymer blends as mucoadhesive/bioadhesive device for sustain drug release in stomach will be able to benefit the treatment of *H. pylori* which is localized in stomach. This strategy should be more advantage than using conventional therapy that needs to administer high amount of drug and requires the re-released of drug to stomach after absorption.

References

1. Burgalassi, S.; Panichi, L.; Saettone, M. F.; Jacobsen, J.; Rassing, M. R. Development and in vitro/in vivo testing of mucoadhesive buccal patches releasing benzydamine and lidocaine. *Int J Pharm* **1996,** 133, 1-7.

2. Perioli, L.; Ambrogi, V.; Rubini, D.; Giovagnoli, S.; Ricci, M.; Blasi, P.; Rossi, C. Novel mucoadhesive buccal formulation containing metronidazole for the treatment of periodontal disease. *J Control Release* **2004,** 95, 521-533.

3. Vishnu, Y. V.; Chandrasekhar, K.; Ramesh, G.; Rao, Y. M. Development of mucoadhesive patches for buccal administration of carvedilol. *Curr Drug Deliv* **2007,** 4, 27-39.

4. Jones, D. S.; Woolfson, A. D.; Djokic, J. Texture profile analysis of bioadhesive polymeric semisolids: mechanical characterization and investigation of interactions between formulation components. *J Appl Polym Sci* **1996,** 61, 2229-2234.

5. Eaimtrakarn, S.; Itoh, Y.; Kishimoto, J.-i.; Yoshikawa, Y.; Shibata, N.; Takada, K. Retention and transit of intestinal mucoadhesive films in rat small intestine. *Int J Pharm* **2001,** 224, 61-67.

6. Vasir, J. K.; Tambwekar, K.; Garg, S. Bioadhesive microspheres as a controlled drug delivery system. *Int J Pharm* **2003,** 255, 13-32.

7. Khoo, C. G. L.; Frantzich, S.; Rosinski, A.; Sjostrom, M.; Hoogstraate, J. Oral gingival delivery systems from chitosan blends with hydrophilic polymers. *Eur J Pharm Biopharm* **2003,** 55, 47-56.

8. Lu, L.; Peng, F.; Jiang, Z.; Wang, J. Poly(vinyl alcohol)/chitosan blend membranes for pervaporation of benzene/cyclohexane mixtures. *J Appl Polym Sci* **2006,** 101, 167–173.

9. Patel, V. M.; Prajapati, B. G.; Patel, M. M. Design and characterization of chitosan-containing mucoadhesive buccal patches of propranolol hydrochloride. *Acta Pharm* **2007,** 57, 61–72.

10. Karavas, E.; Georgarakis, E.; Bikiaris, D. Adjusting drug release by using miscible polymer blends as effective drug carries. *J Therm Anal Cal* **2006,** 84, 125-133.

11. Marsano, E.; Vicini, S.; Skopinska, J.; Wisniewski, M.; Sionkowska, A. Chitosan and poly(vinyl pyrrolidone): compatibility and miscibility of blends. *Macromol Symp* **2004,** 218, 251-260.

12. Yilmaz, E.; Ozalp, D.; Yilmaz, O. Miscibility study of chitosan/poly(vinylpyrrolidone) blends in dilute solution. *Int J Polym Anal Ch* **2005,** 10, 329–339.

13. Abou-Aiad, T. H. M.; Abd-El-Nour, K. N.; Hakim, I. K.; Elsabee, M. Z. Dielectric and interaction behavior of chitosan/polyvinyl alcohol and chitosan/polyvinyl pyrrolidone blends with some antimicrobial activities. *Polymer* **2006,** 47, 379–389.

14. Sakurai, K.; Maegawa, T.; Takahashi, T. Glass transition temperature of chitosan and miscibility of chitosan/poly(N-vinyl pyrrolidone) blends. *Polymer* **2000,** 41, 7051–7056.

15. Sandoval, C.; Castro, C.; Gargallo, L.; Radic, D.; Freire, J. Specific interactions in blends containing chitosan and functionalized polymers. Molecular dynamics simulations. *Polymer* **2005,** 46, 10437-10442.

16. Pandit, S. A.; Bostick, D.; Berkowitz, M. L. Molecular dynamics simulation of a dipalmitoylphosphatidylcholine bilayer with NaCl. *Biophys J* **2003,** 84, 3743-3750.

17. Suknuntha, K.; Tantishaiyakul, V.; Vao-Soongnern, V.; Espidel, Y.; Cosgrove, T. Molecular modeling simulation and experimental measurements to characterize chitosan and poly(vinyl pyrrolidone) blend interactions. *J Polym Sci Pol Phys* **2008,** 46, 1258-1264.

18. Hassan, E. E.; Gallo, J. M. A simple rheological method for the *in vitro* assessment of mucin-polymer bioadhesive bond strength. *Pharm Res* **1990,** 7, 491-495.

19. Sun, H. COMPASS: an ab Initio force-field optimized for condensed-phase applications-overview with details on alkane and benzene compounds. *J Phys Chem B* **1998,** 102, 7338-7364.

20. Prathab, B.; Aminabhavi, T. M. Atomistic simulations to compute surface properties of poly(N-vinyl-2-pyrrolidone) (PVP) and blends of PVP/chitosan. *Langmuir* **2007,** 23, 5439-5444.

21. Chen, C.; Dong, L.; Cheung, M. K. Preparation and characterization of biodegradable poly(L-lactide)/chitosan blends. *Eur Polym J* **2005,** 41, 958–966.

22. Xu, W.; Luo, Q.; Wang, H.; Francesconi, L. C.; Stark, R. E.; Akins, D. L. Polyoxoanion occluded within modified MCM-41: spectroscopy and structure. *J Phys Chem B* **2003,** 107, 497-501.

23. Miller, J. M.; Lakshmi, L. J. Spectroscopic characterization of sol-gel-derived mixed oxides. *J Phys Chem B* **1998,** 102, 6465-6470.

24. Heux, L.; Brugnerotto, J.; Desbrieres, J.; Versali, M.-F.; Rinaudo, M. Solid state NMR for determination of degree of acetylation of chitin and chitosan. *Biomacromolecules* **2000,** 1, 746-751.

25. Miyoshi, T.; Takegoshi, K.; Hikichi, K. High-resolution solid state 13C n.m.r, study of the interpolymer interaction, morphology and chain dynamics of the poly(acrylic acid)/poly(ethylene oxide) complex. *Polymer* **1997,** 38, 2315-2320.

26. Jawalkar, S. S.; Raju, K. V. S. N.; Halligudi, S. B.; Sairam, M.; Aminabhavi, T. M. Molecular modeling simulations to predict compatibility of poly(vinyl alcohol) and chitosan blends: a comparison with experiments. *J Phys Chem B* **2007,** 111, 2431-2439.

27. *The Merck Index*. 15th ed.; Whitehouse Station, NJ: Merck: 2001.

28. Wikman, A.; Karlsson, J.; Carlstedt, I.; Artursson, P. A drug absorption model based on the mucus layer producing human intestinal goblet cell line HT29-H *Pharm Res* **1993,** 10, 843-852.

Acknowledgements

This research work was supported by these following grants:

1. Prince of Songkla University through Grant No. PHA50162
2. The Thailand Research Fund through the Royal Golden Jubilee Ph.D. Program through Grant No. PHD/5GPS/47/D1 for Krit Suknuntha
3. Ministry of Education through the Tailor-made Medicine for the Enhancement of Thailand Competitiveness Project for Traveling grant and Dr. Youssef Espidel and Prof. Terrence Cosgrove for performing ^{13}C CP/MAS NMR spectra of chitosan, PVP and 50/50 PVP/chitosan blend
4. The National Nanotechnology Center (NANOTEC), National Science and Technology Development Agency (NSTDA), Ministry of Science and Technology through its National Nanoscience Consortium (CNC) and Asst Prof Visit Vao-Soongnern for providing Materails Studio program and support in molecular dynamic simulation part.

Remarks

1. Due to time consuming and lack of specific molecular structures of other polymers, only the interaction between chitosan and PVP blend at 50/50 ratio was investigated using molecular dynamic simulation.

2. A part of this work was prepared as a manuscript entitle "Molecular modeling simulation and experimental measurements to characterize chitosan and poly(vinyl pyrrolidone) blend interactions" and it was published in the Journal of Polymer Science Part B: Polymer Physics **2008,** 46, 1258-1264.

3. Besides above mentioned polymer blends, trimethylchitosan (TMC) was also synthesis as previously reported.

Synthesis of N-trimethylChitosan (TMC)

N-trimethylchitosan was synthesized as previously described[1]. In brief, A mixture of 2 g of sieved chitosan (93% deacetylated), 4.8 g of sodium iodide, 11 mL of a 15% aqueous sodium hydroxide solution and 11.5 mL of methyl iodide in 80 mL of 1-methyl-2-pyrrolidinone was stirred on a water bath of 60°C for 1 h. Special care was taken to keep the methyl iodide in the reaction mixture by using a Liebig condenser. The product was precipitated using ethanol and thereafter isolated by centrifugation. The N-trimethyl chitosan iodide obtained after this first step was washed twice with ether on a glass filter to remove the ethanol. It was dissolved in 80 mL of 1-methyl-2-pyrrolidinone and heated to 6O°C, thus removing most of the absorbed ether. Subsequently, 4.8 g of NaI, 11 mL of 15% NaOH solution and 7 mL of methyl iodide were added with rapid stirring and the mixture was heated on a water bath at 60°C for 30 min. An additional 2 mL of methyl iodide and 0.6 g of NaOH pellets were added and the stirring was continued for 1 h. The product, prepared as described above, was dissolved in 40 mL of a 10% NaCl aqueous solution, instead of HCl, to exchange the iodide. The polymer was precipitated with ethanol, isolated by centrifugation and thoroughly washed with ethanol and ether. In vacuo drying yielded a white, water-soluble powder.

Due to the problem in texture analysis of this TMC film, this material is not further studied in this project.

Reference

1. Sieval, A. B.; Thanou, M.; Kotze, A. F.; Verhoef, J. C.; Brussee, J.; Junginger, H. E. Preparation and NMR characterization of highly substituted N-trimethyl chitosan chloride. *Carbohyd Polym* **1998,** 36, 157-165.

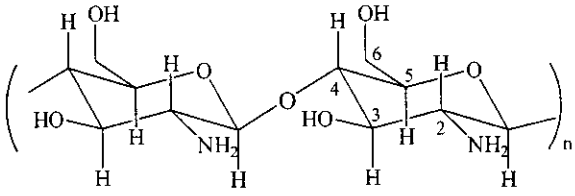

Chitosan

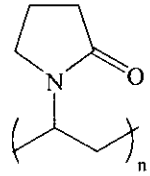

Poly(vinyl pyrrolidone)

Figure 1. Structures of chitosan and poly(vinyl pyrrolidone)

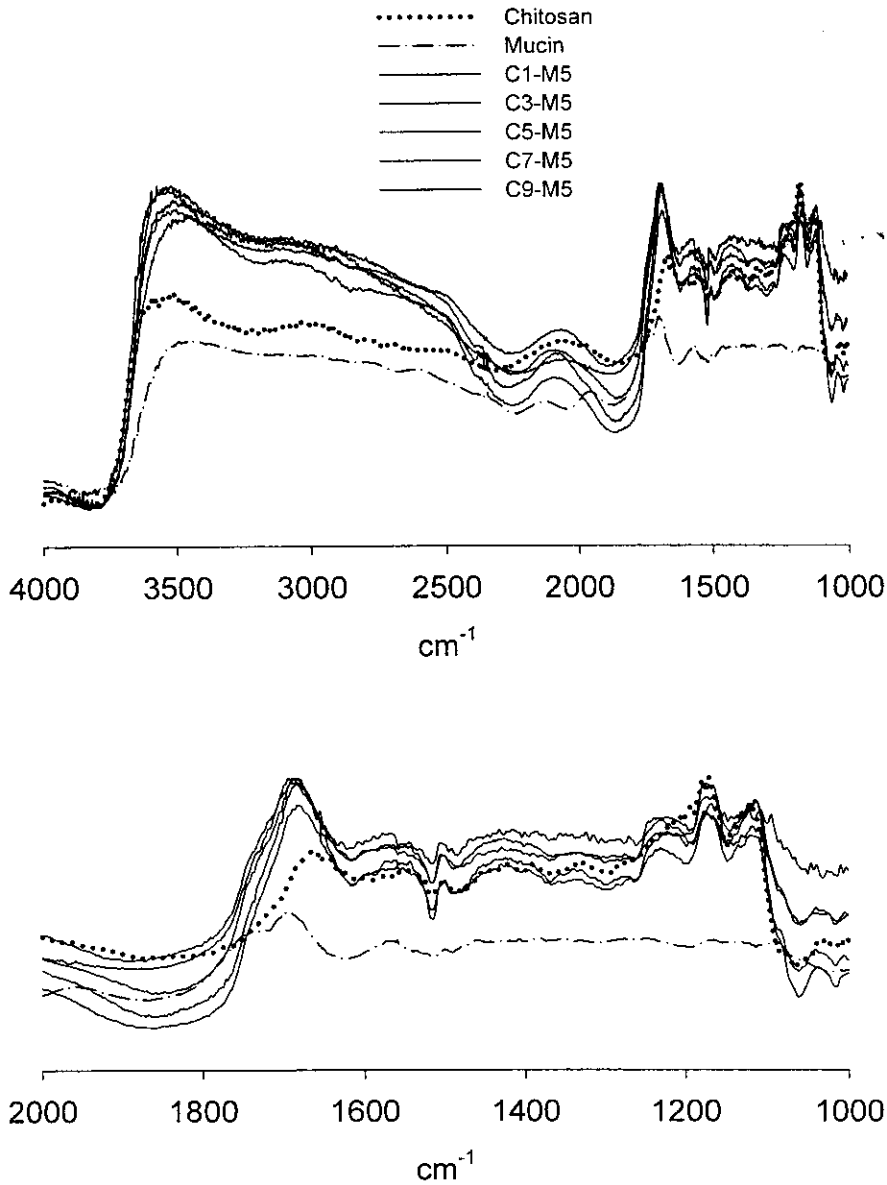

Figure 2 DRIFTS spectra of chitosan (C), mucin (M), and mixtures of C:M at volume ratios of 1:5 (C1-M5), 3:5 (C3-M5), 5:5 (C5-M5), 7:5 (C7-M5) and 9:5 (C9-M5).

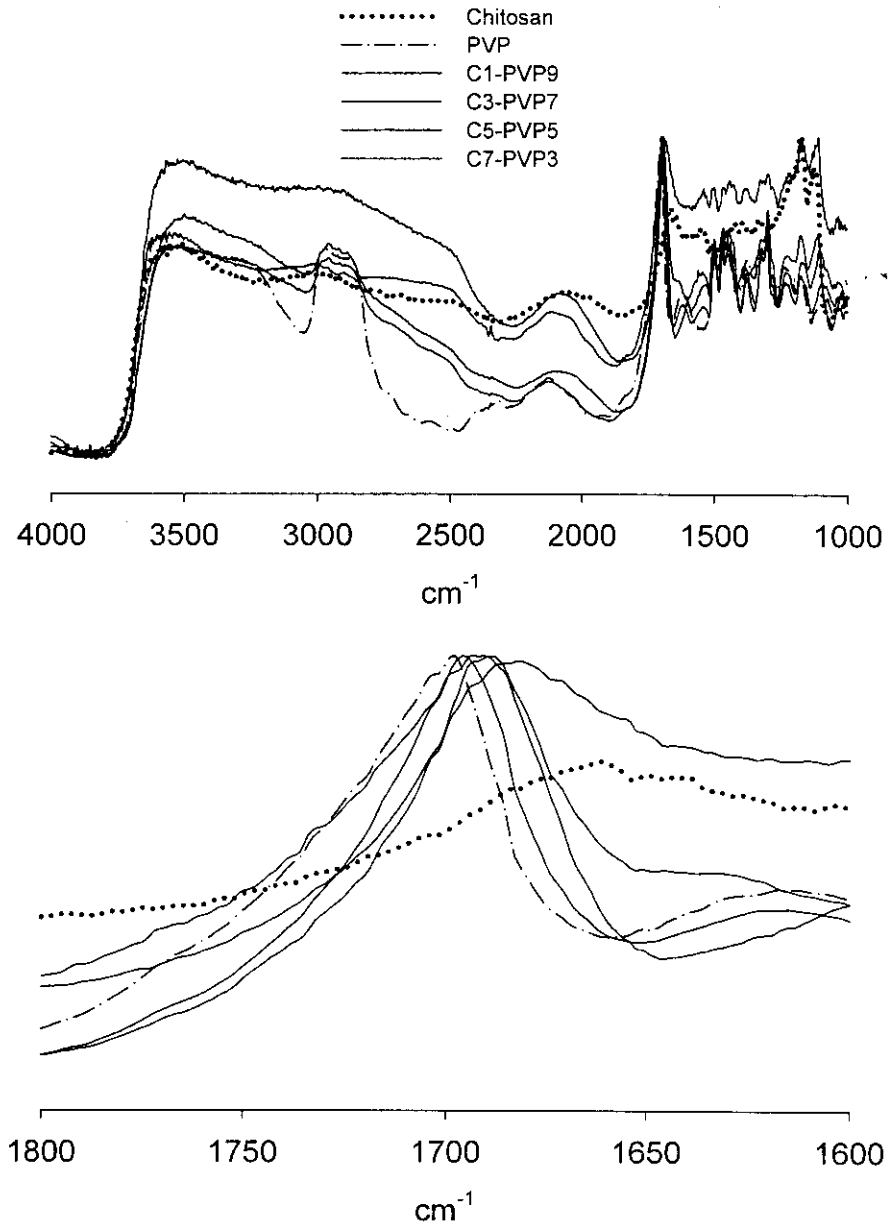

Figure 3 DRIFTS spectra of chitosan (C), poly(vinyl pyrrolidone) (PVP), and mixtures of C:PVP at volume ratios of 1:9 (C1-PVP9), 3:7 (C3-PVP7), 5:5 (C5-PVP5), and 7:3 (C7-PVP3).

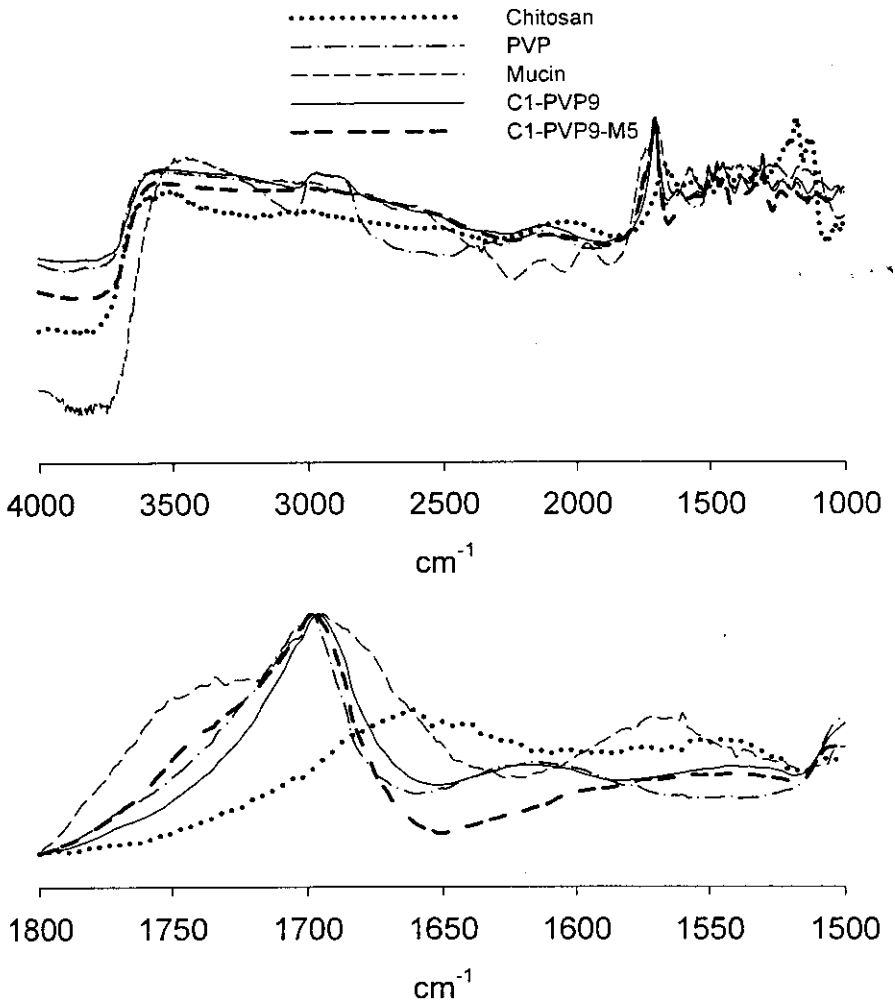

Figure 4 DRIFTS spectra of chitosan (C), poly(vinyl pyrrolidone) (PVP), mucin (M), mixture of C:PVP at volume ratio of 1:9 (C1-PVP9), and mixture of C:PVP:M at volume ratio of 1:9:5 (C1-PVP9:M5).

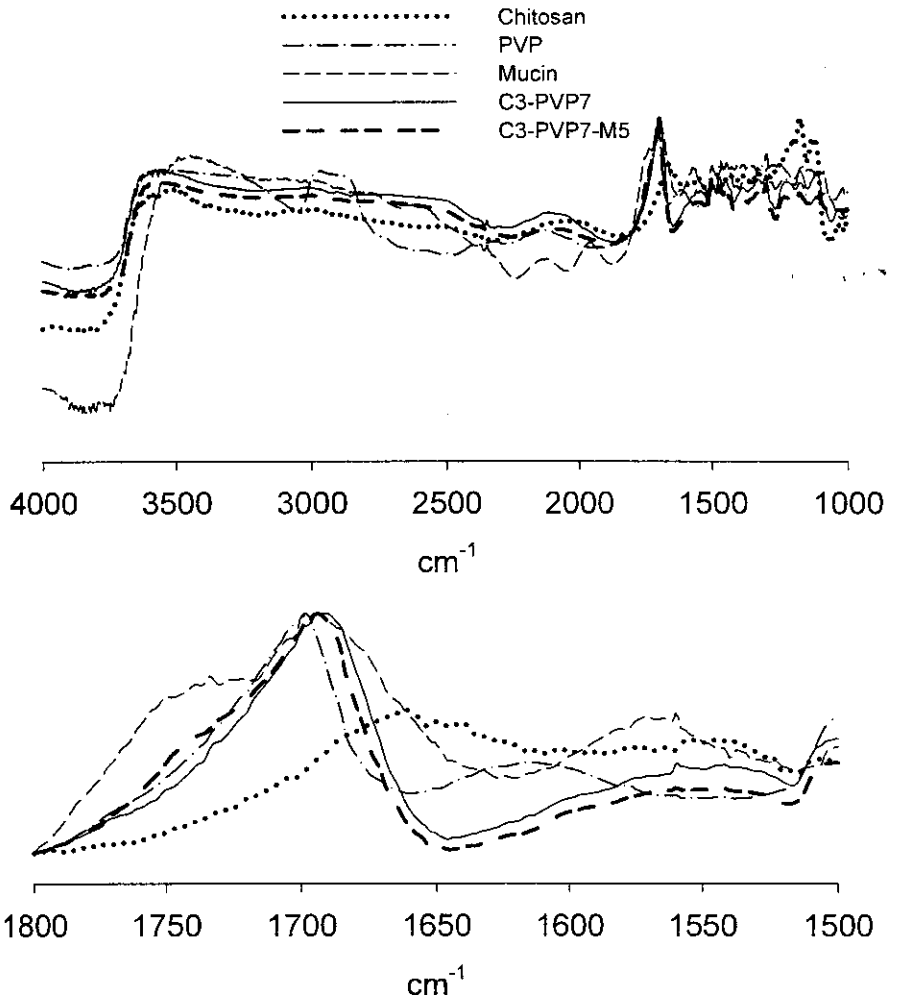

Figure 5 DRIFTS spectra of chitosan (C), poly(vinyl pyrrolidone) (PVP), mucin (M), mixture of C:PVP at volume ratio of 3:7 (C3-PVP7), and mixture of C:PVP:M at volume ratio of 3:7:5 (C3-PVP7:M5).

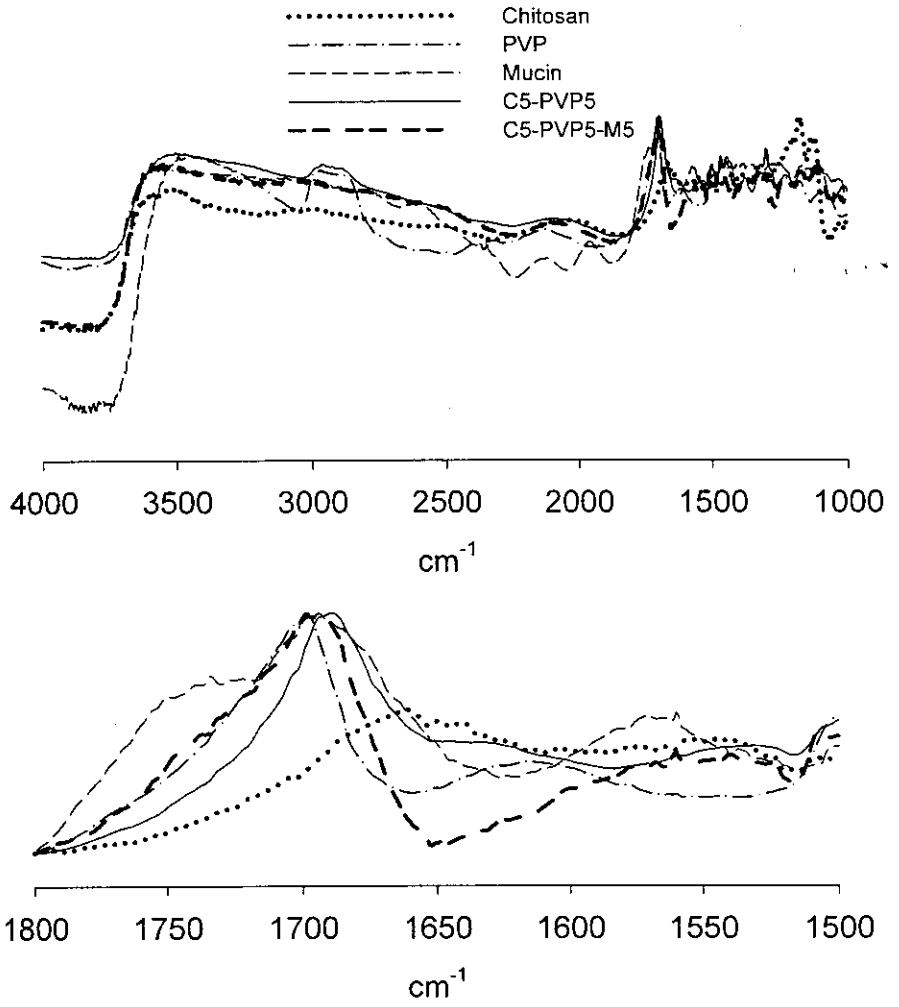

Figure 6 DRIFTS spectra of chitosan (C), poly(vinyl pyrrolidone) (PVP), mucin (M), mixture of C:PVP at volume ratio of 5:5 (C5-PVP5), and mixture of C:PVP:M at volume ratio of 5:5:5 (C5-PVP5:M5).

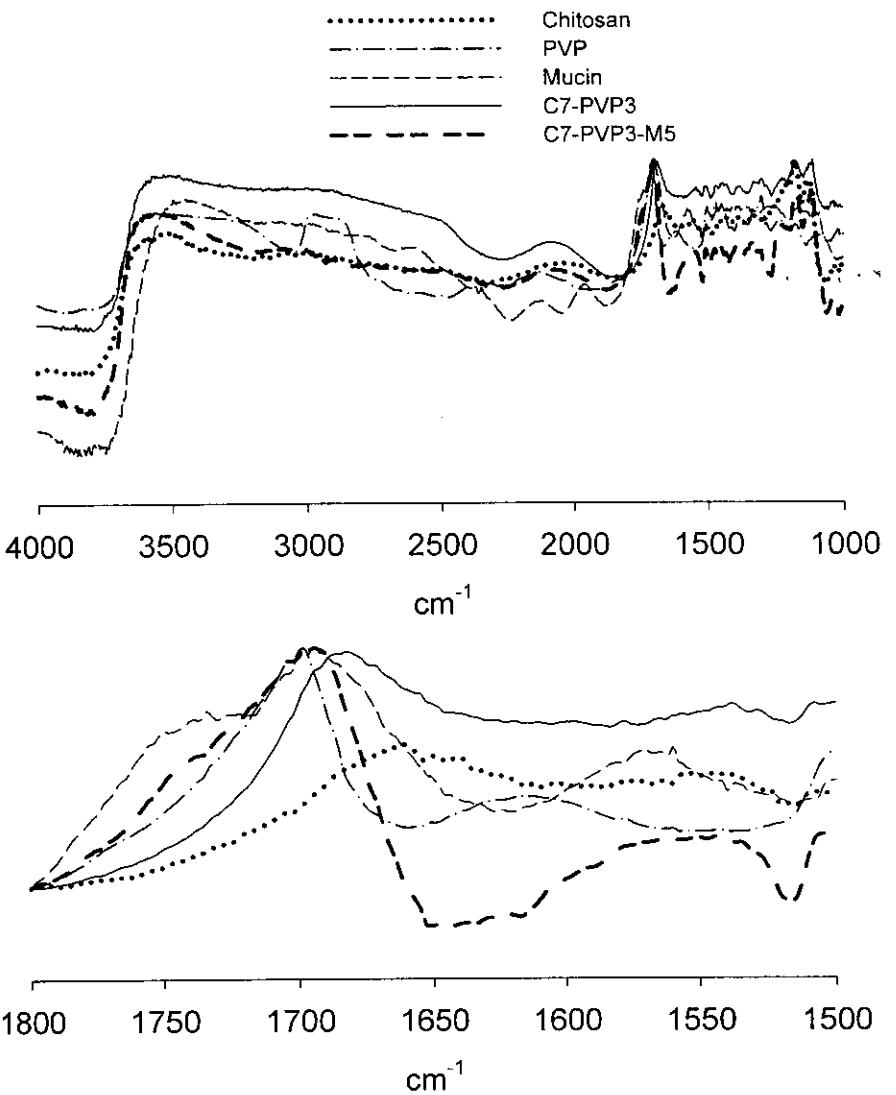

Figure 7 DRIFTS spectra of chitosan (C), poly(vinyl pyrrolidone) (PVP), mucin (M), mixture of C:PVP at volume ratio of 7:3 (C7-PVP3), and mixture of C:PVP:M at volume ratio of 7:3:5 (C7-PVP3:M5).

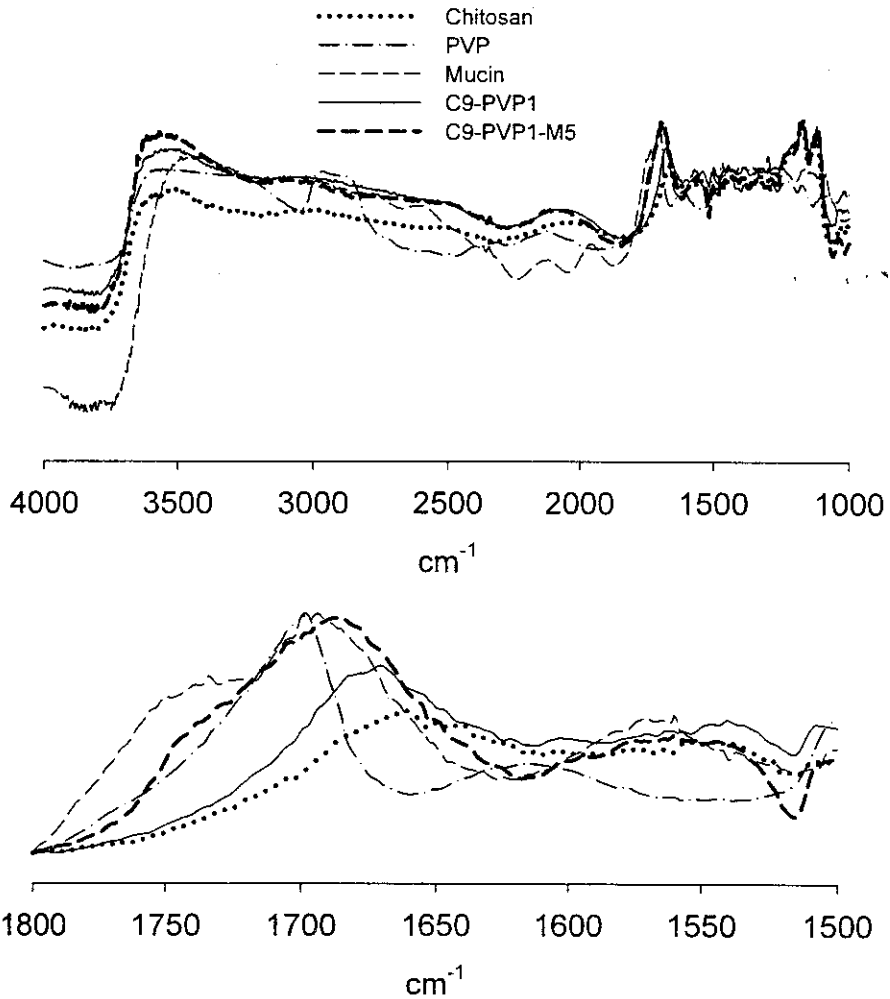

Figure 8 DRIFTS spectra of chitosan (C), poly(vinyl pyrrolidone) (PVP), mucin (M), mixture of C:PVP at volume ratio of 9:1 (C9-PVP1), and mixture of C:PVP:M at volume ratio of 9:1:5 (C9-PVP1:M5).

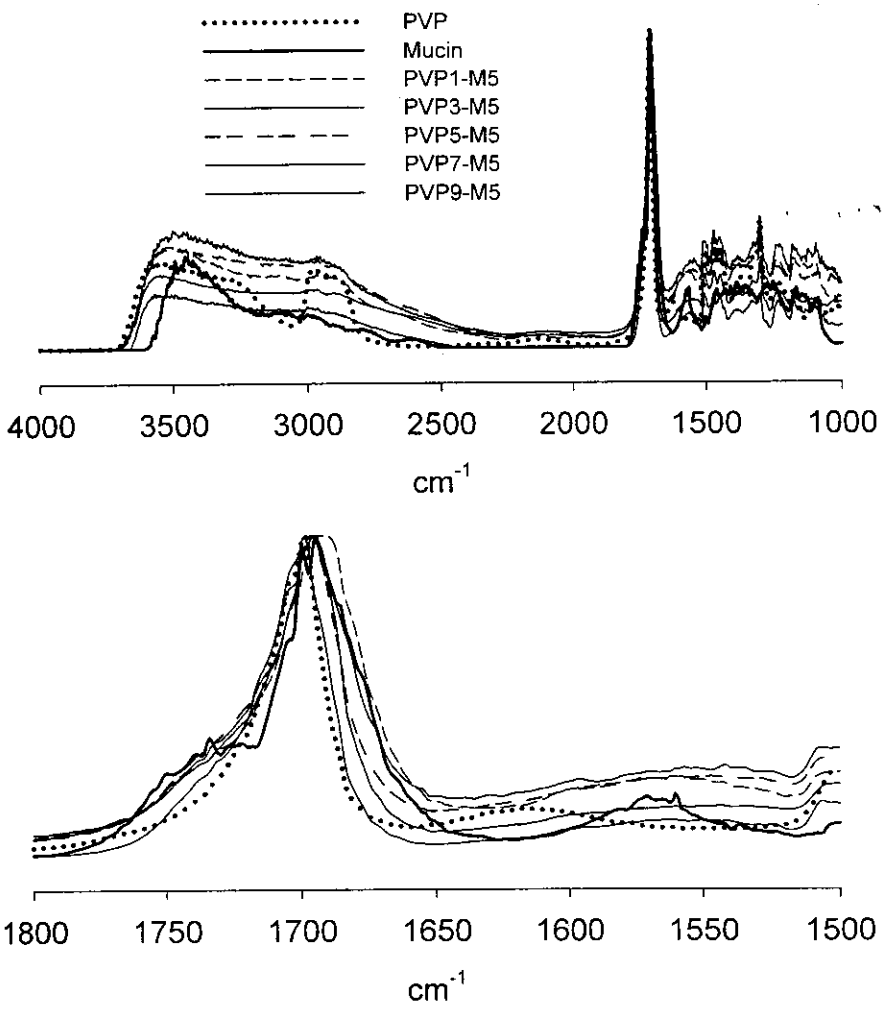

Figure 9 DRIFTS spectra of poly(vinyl pyrrolidone) (PVP), mucin (M), and mixtures of PVP:M at volume ratios of 1:5 (PVP1-M5), 3:5 (PVP3-M5), 5:5 (PVP5-M5), 7:5 (PVP7-M5) and 9:5 (PVP9-M5).

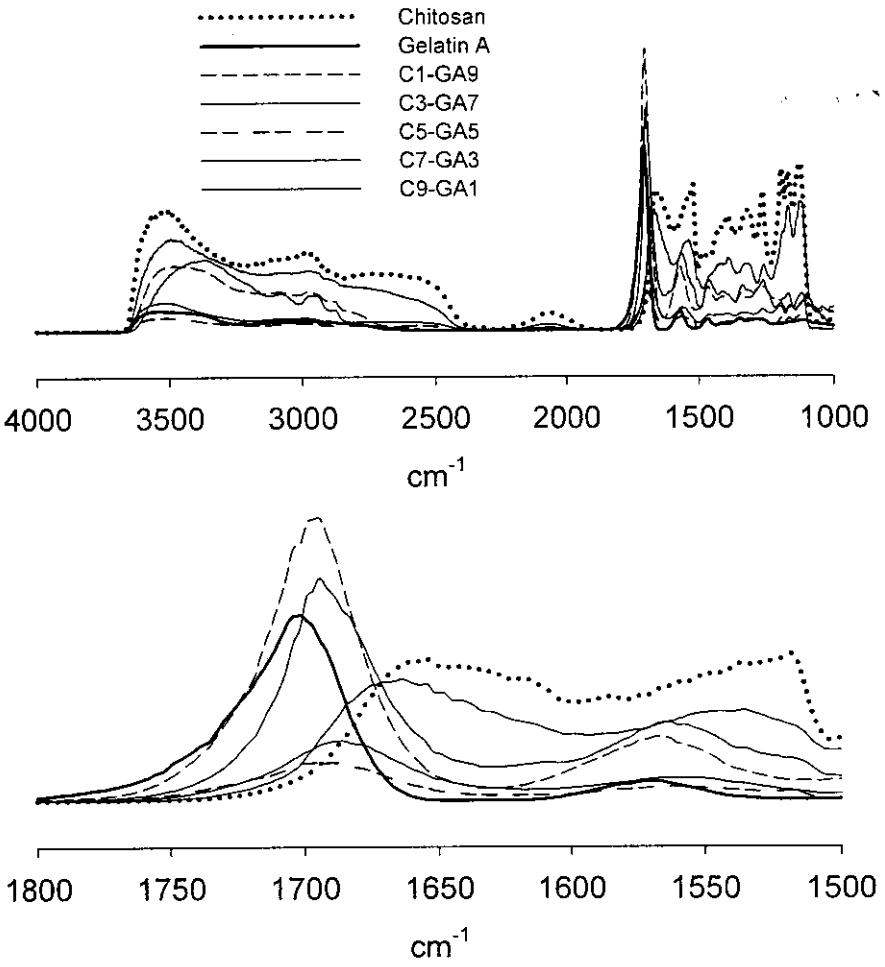

Figure 10 DRIFTS spectra of chitosan (C), gelatin A (GA), and mixtures of C:GA at volume ratios of 1:9 (C-GA9), 3:7 (C3-GA7), 5:5 (C5-GA5), 7:3 (C7-GA3) and 9:1 (C9-GA1).

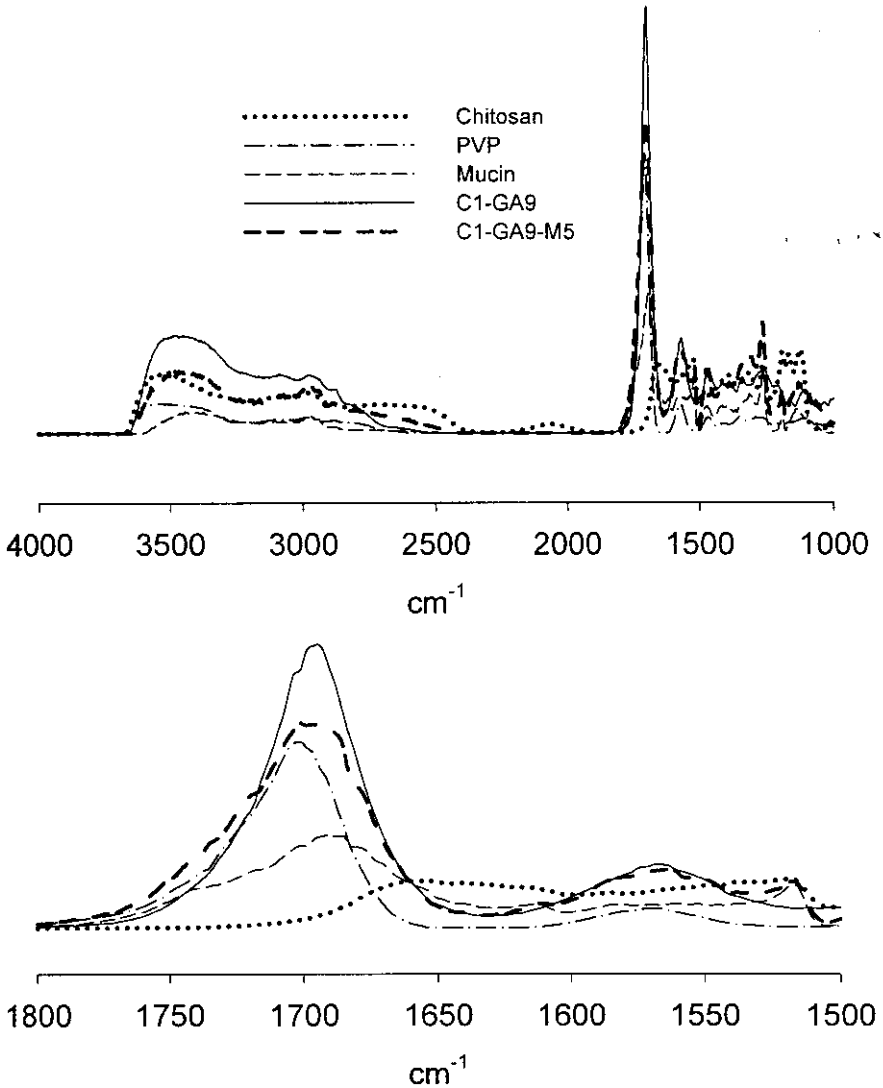

Figure 11 DRIFTS spectra of chitosan (C), gelatin A (GA), mucin (M), mixture of C:GA at volume ratio of 1:9 (C1-GA9), and mixture of C:GA:M at volume ratio of 1:9:5 (C1-GA9:M5).

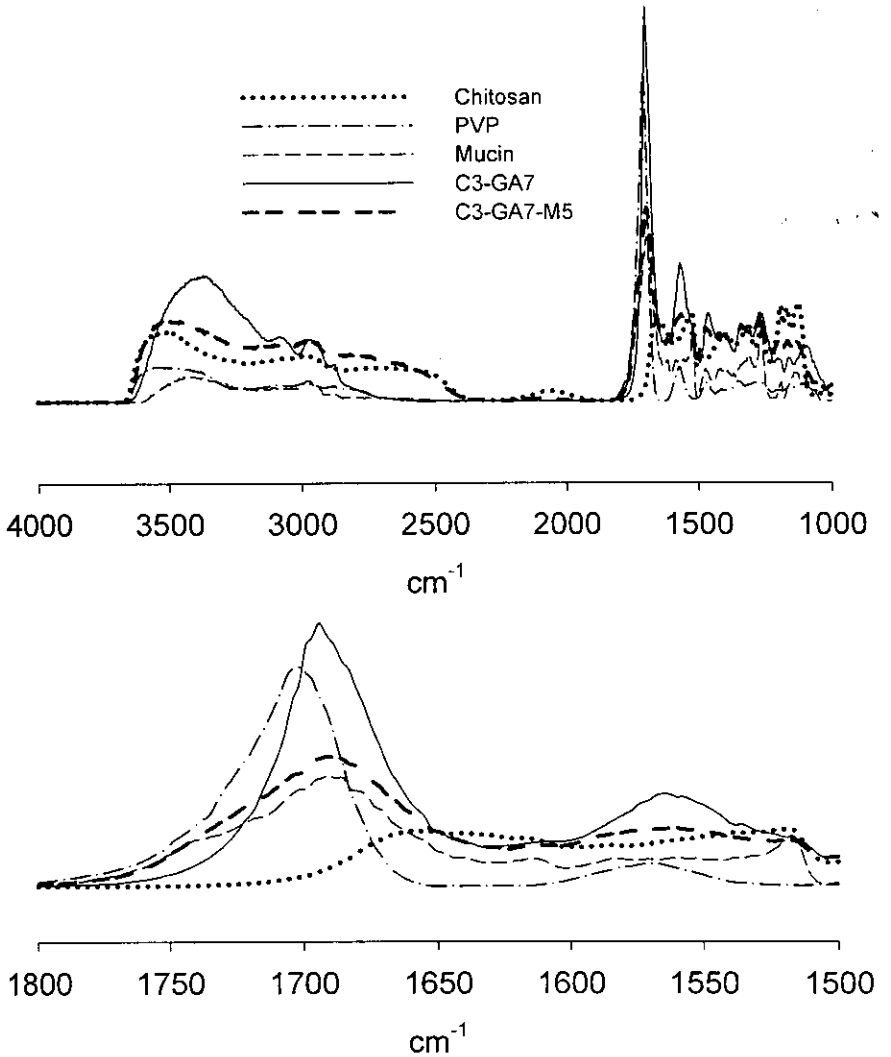

Figure 12 DRIFTS spectra of chitosan (C), gelatin A (GA), mucin (M), mixture of C:GA at volume ratio of 3:7 (C3-GA7), and mixture of C:GA:M at volume ratio of 3:7:5 (C3-GA7:M5).

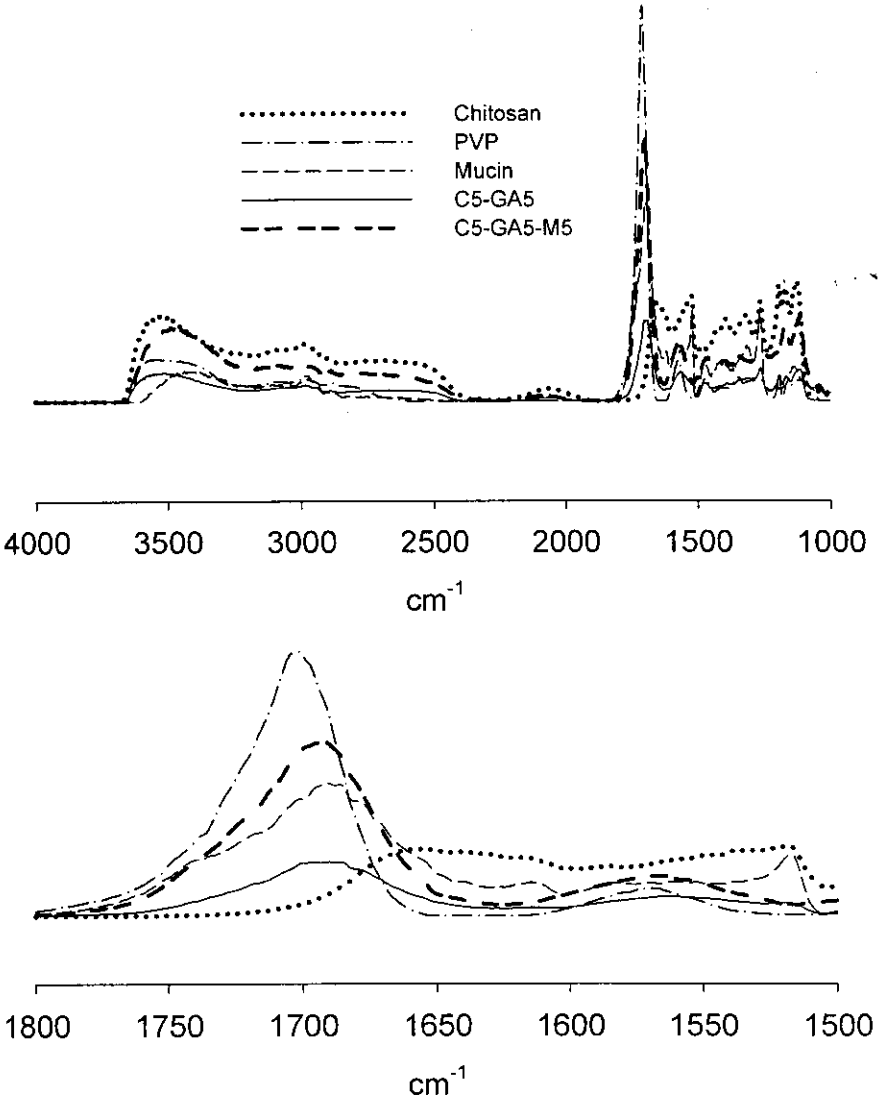

Figure 13 DRIFTS spectra of chitosan (C), gelatin A (GA), mucin (M), mixture of C:GA at volume ratio of 5:5 (C5-GA5), and mixture of C:GA:M at volume ratio of 5:5:5 (C5-GA5:M5).

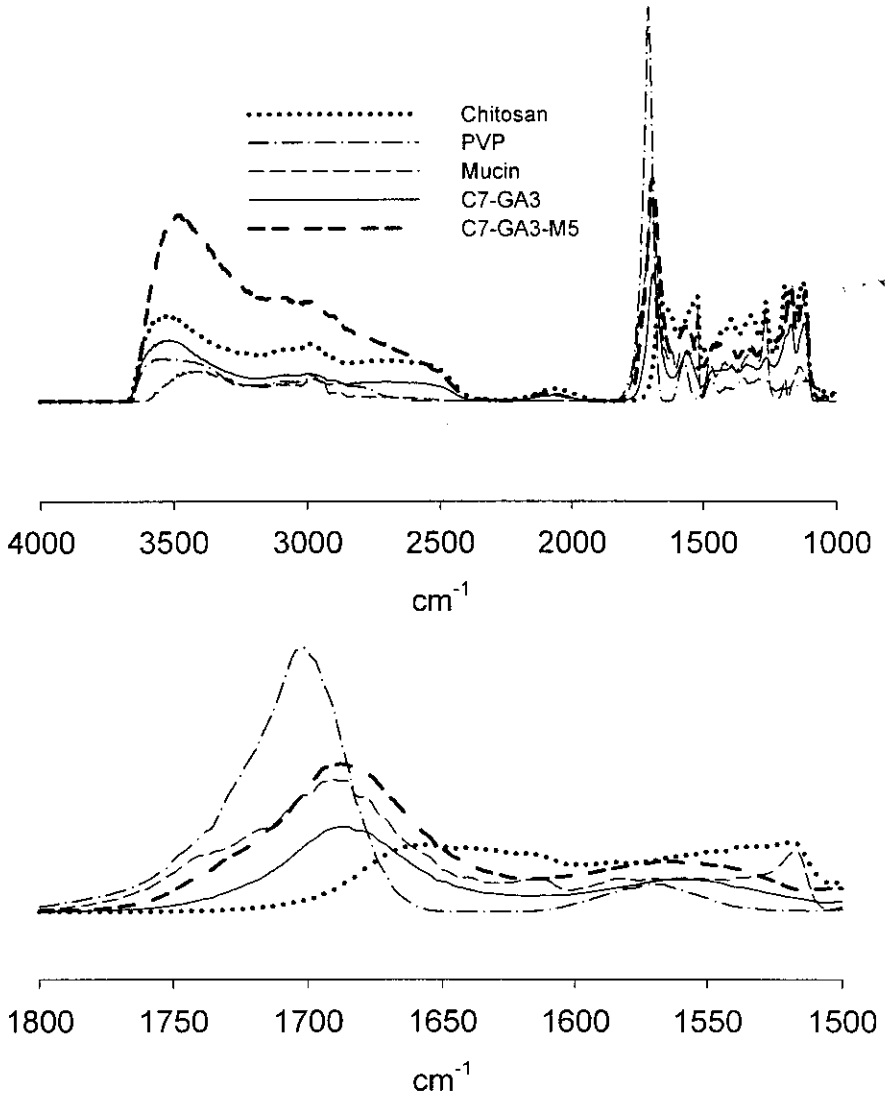

Figure 14 DRIFTS spectra of chitosan (C), gelatin A (GA), mucin (M), mixture of C:GA at volume ratio of 7:3 (C7-GA3), and mixture of C:GA:M at volume ratio of 7:3:5 (C7-GA3:M5).

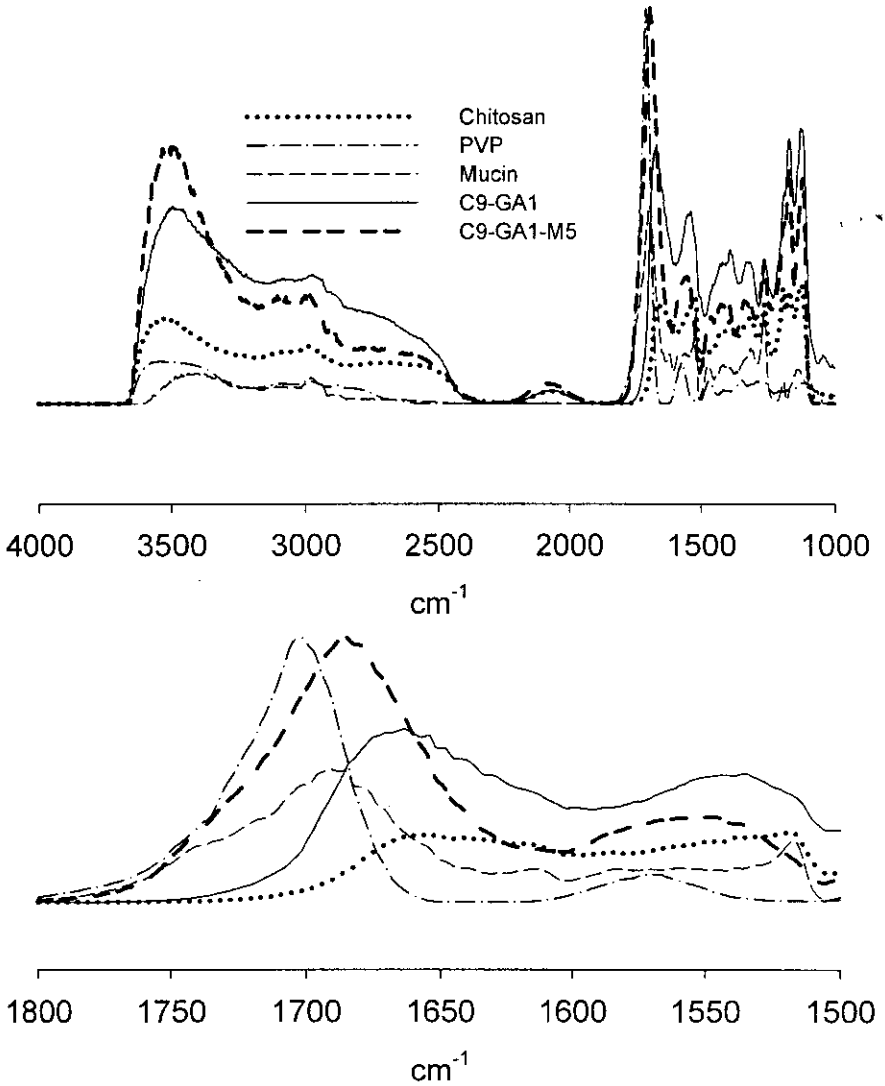

Figure 15 DRIFTS spectra of chitosan (C), gelatin A (GA), mucin (M), mixture of C:GA at volume ratio of 9:1 (C9-GA1), and mixture of C:GA:M at volume ratio of 9:1:5 (C9-GA1:M5).

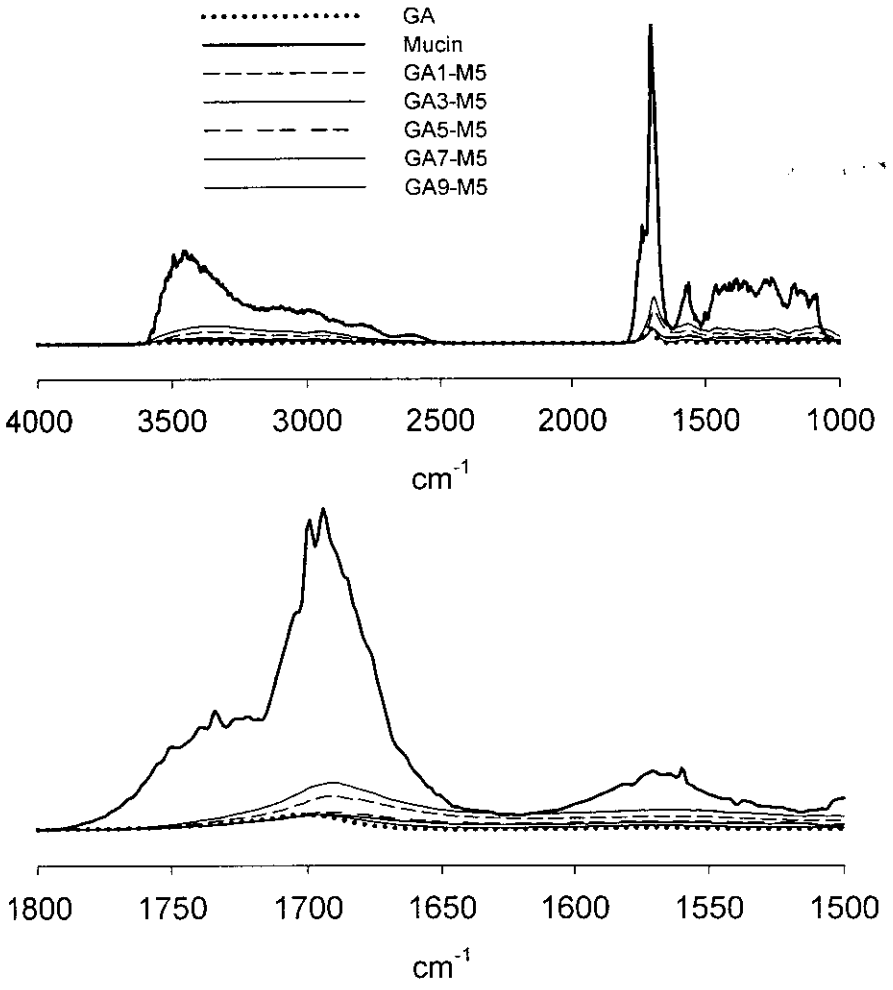

Figure 16 DRIFTS spectra of gelatin A (GA), mucin (M), and mixtures of GA:M at volume ratios of 1:5 (GA1-M5), 3:5 (GA3-M5), 5:5 (GA5-M5), 7:5 (GA7-M5) and 9:5 (GA1-M5).

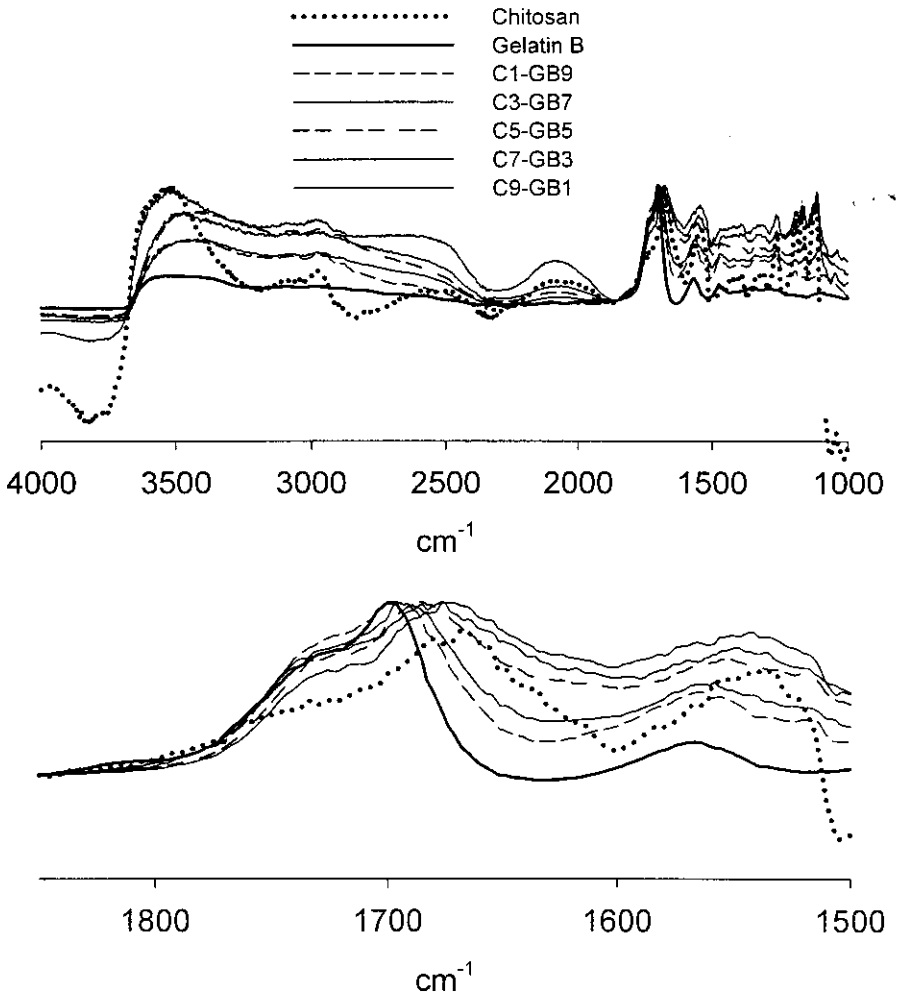

Figure 17 DRIFTS spectra of chitosan (C), gelatin B (GB), and mixtures of C:GB at volume ratios of 1:9 (C1-GB9), 3:7 (C3-GB7), 5:5 (C5-GB5), 7:3 (C7-GB3) and 9:1 (C9-GB1).

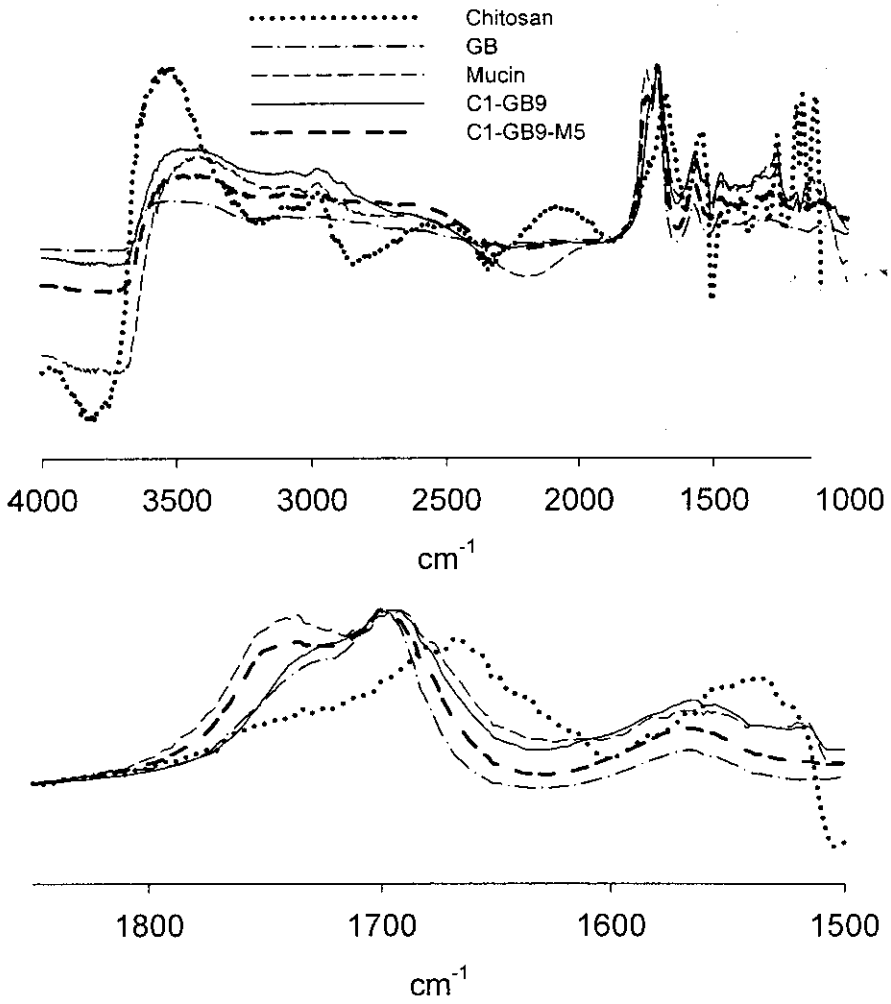

Figure 18 DRIFTS spectra of chitosan (C), gelatin B (GB), mucin (M), mixture of C:GB at volume ratio of 1:9 (C1-GB9), and mixture of C:GB:M at volume ratio of 1:9:5 (C1-GB9:M5).

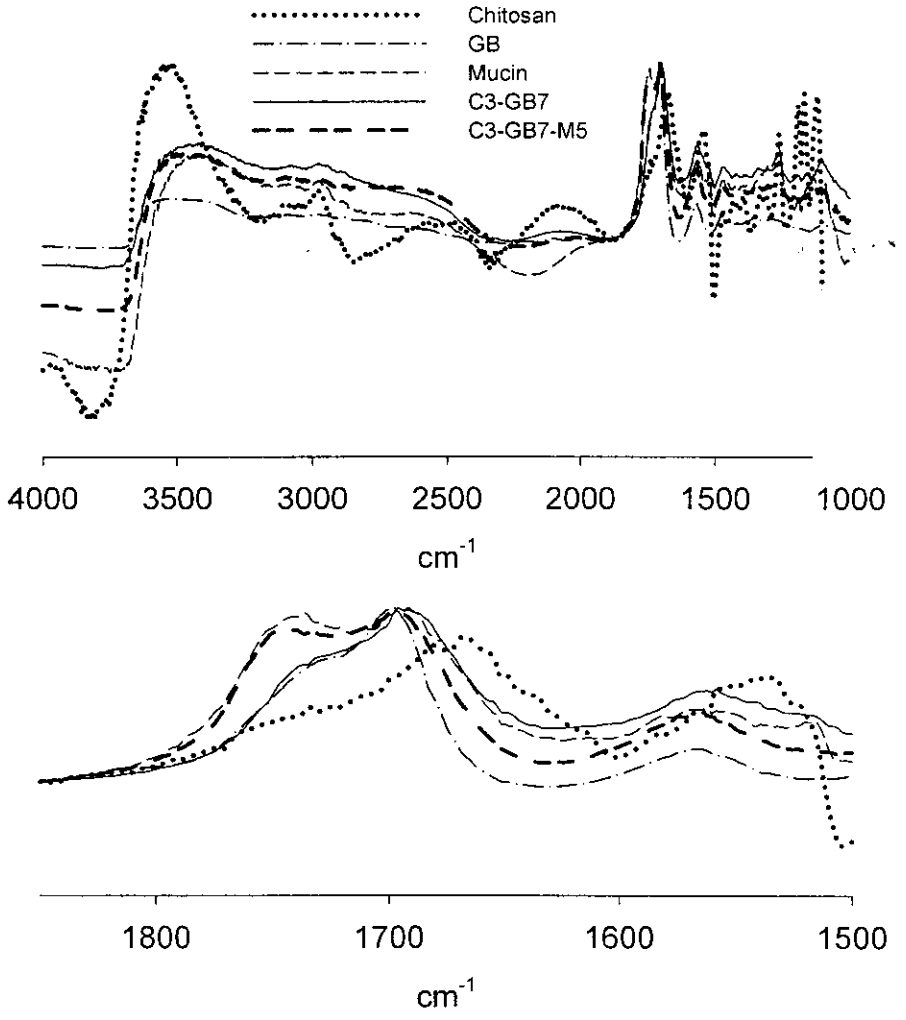

Figure 19 DRIFTS spectra of chitosan (C), gelatin B (GB), mucin (M), mixture of C:GB at volume ratio of 3:7 (C3-GB7), and mixture of C:GB:M at volume ratio of 3:7:5 (C3-GB7:M5).

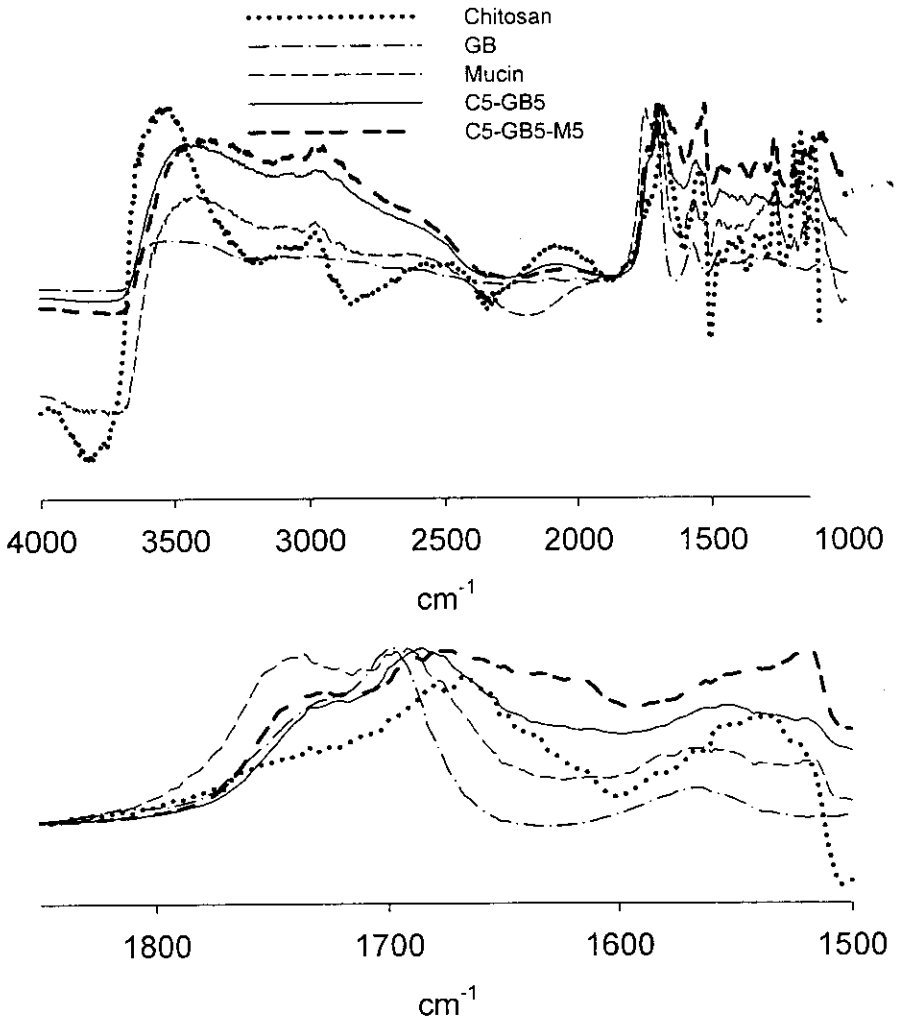

Figure 20 DRIFTS spectra of chitosan (C), gelatin B (GB), mucin (M), mixture of C:GB at volume ratio of 5:5 (C5-GB5), and mixture of C:GB:M at volume ratio of 5:5:5 (C5-GB5:M5).

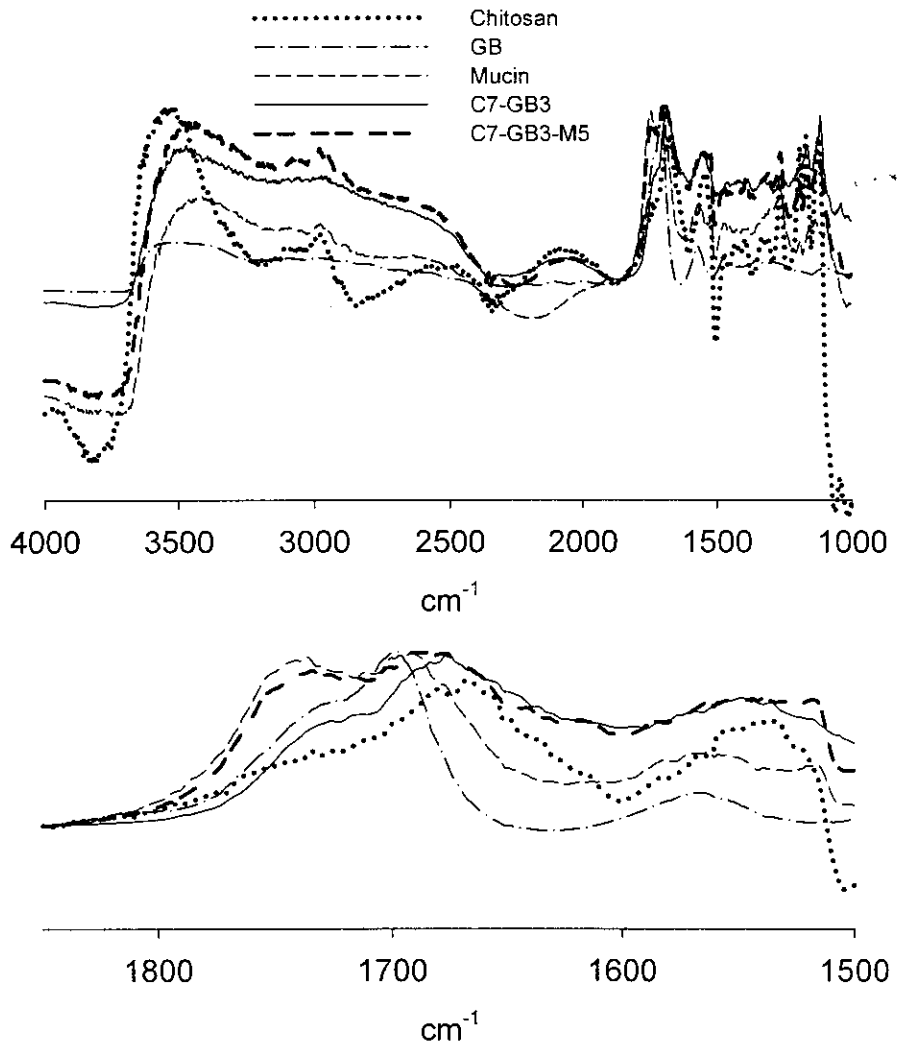

Figure 21 DRIFTS spectra of chitosan (C), gelatin B (GB), mucin (M), mixture of C:GB at volume ratio of 7:3 (C7-GB3), and mixture of C:GB:M at volume ratio of 7:3:5 (C7-GB3:M5).

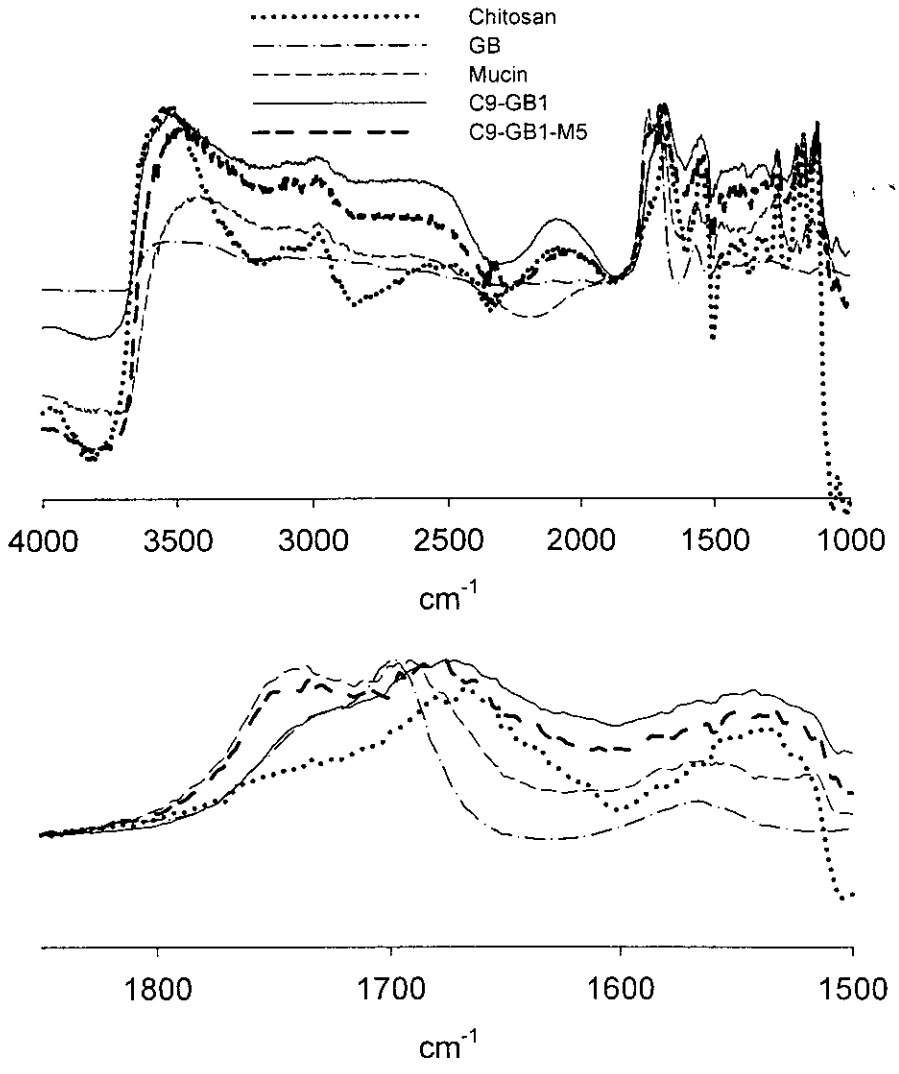

Figure 22 DRIFTS spectra of chitosan (C), gelatin B (GB), mucin (M), mixture of C:GB at volume ratio of 9:1 (C9-GB1), and mixture of C:GB:M at volume ratio of 9:1:5 (C9-GB1:M5).

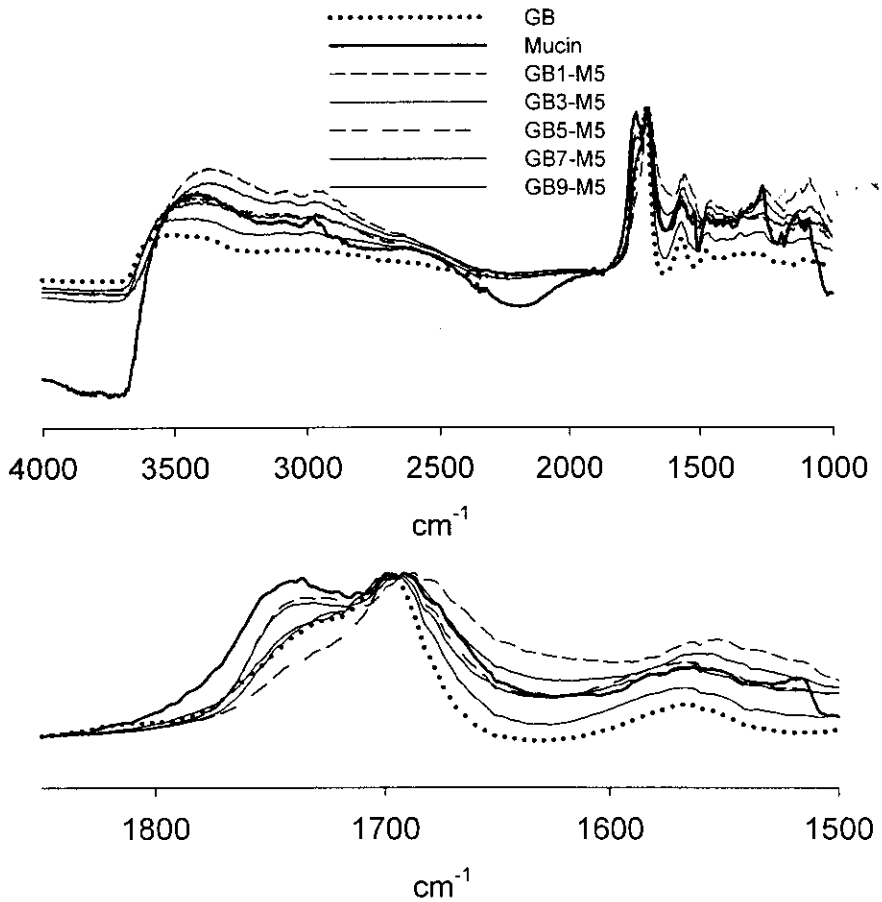

Figure 23 DRIFTS spectra of gelatin B (GB), mucin (M), and mixtures of GB:M at volume ratios of 1:5 (GB1-M5), 3:5 (GB3-M5), 5:5 (GB5-M5), 7:5 (GB7-M5) and 9:5 (GB1-M5).

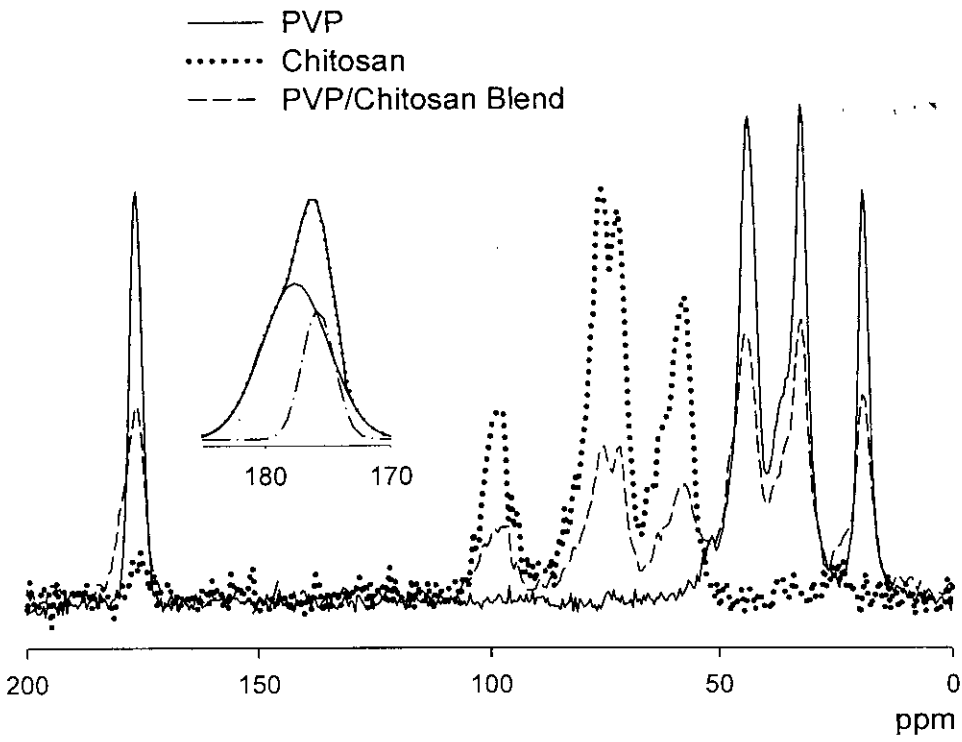

Figure 24 ^{13}C CP/MAS NMR spectra of chitosan, PVP and 50:50 PVP-chitosan blend; inset: the resolved spectrum of C=O band of the 50:50 PVP:chitosan blend.

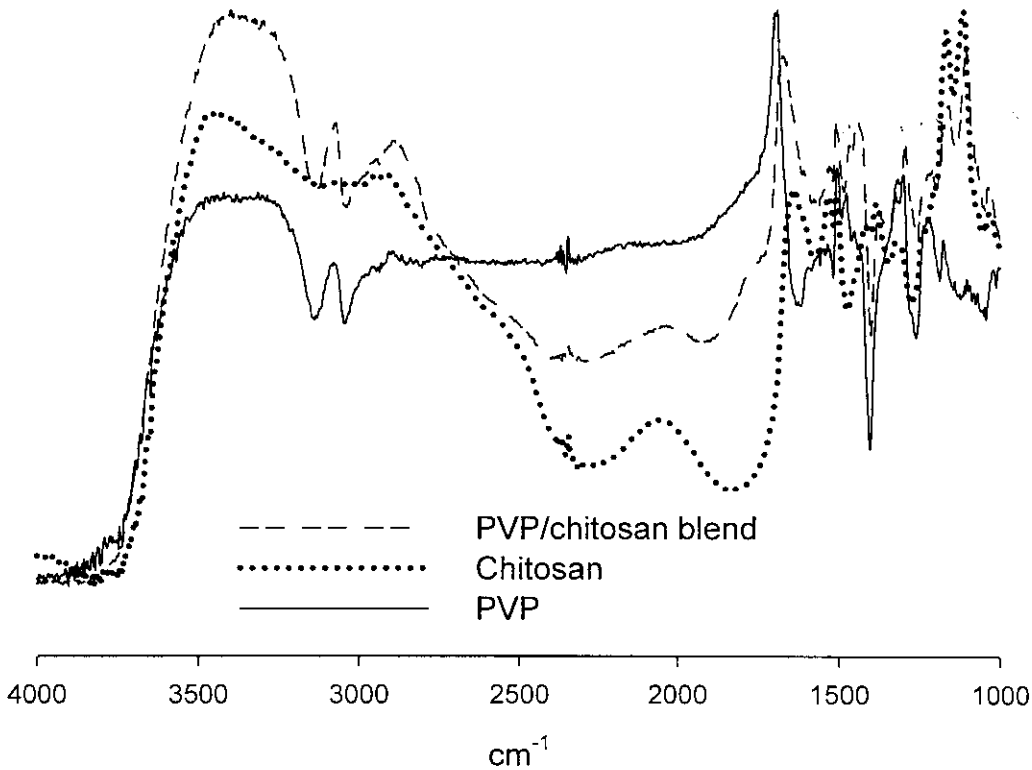

Figure 25 DRIFR spectra of chitosan, PVP and 50:50 PVP-chitosan blend

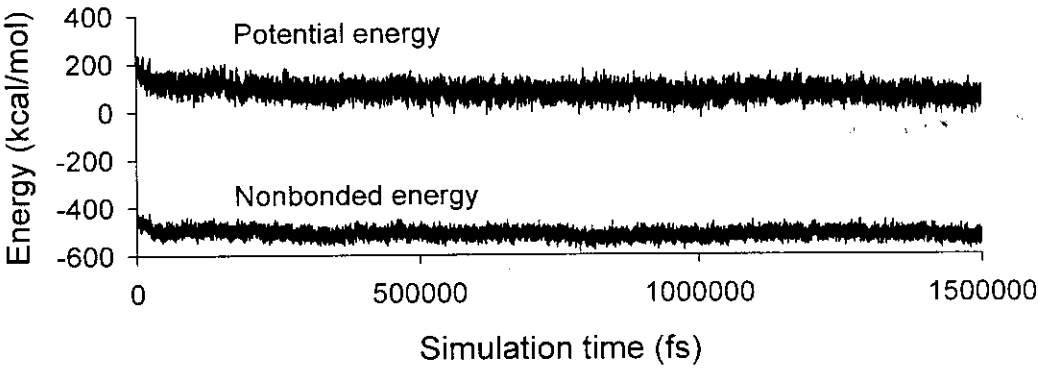

Figure 26 Potential and nonbonded energy vs simulation time of 1500 ps.

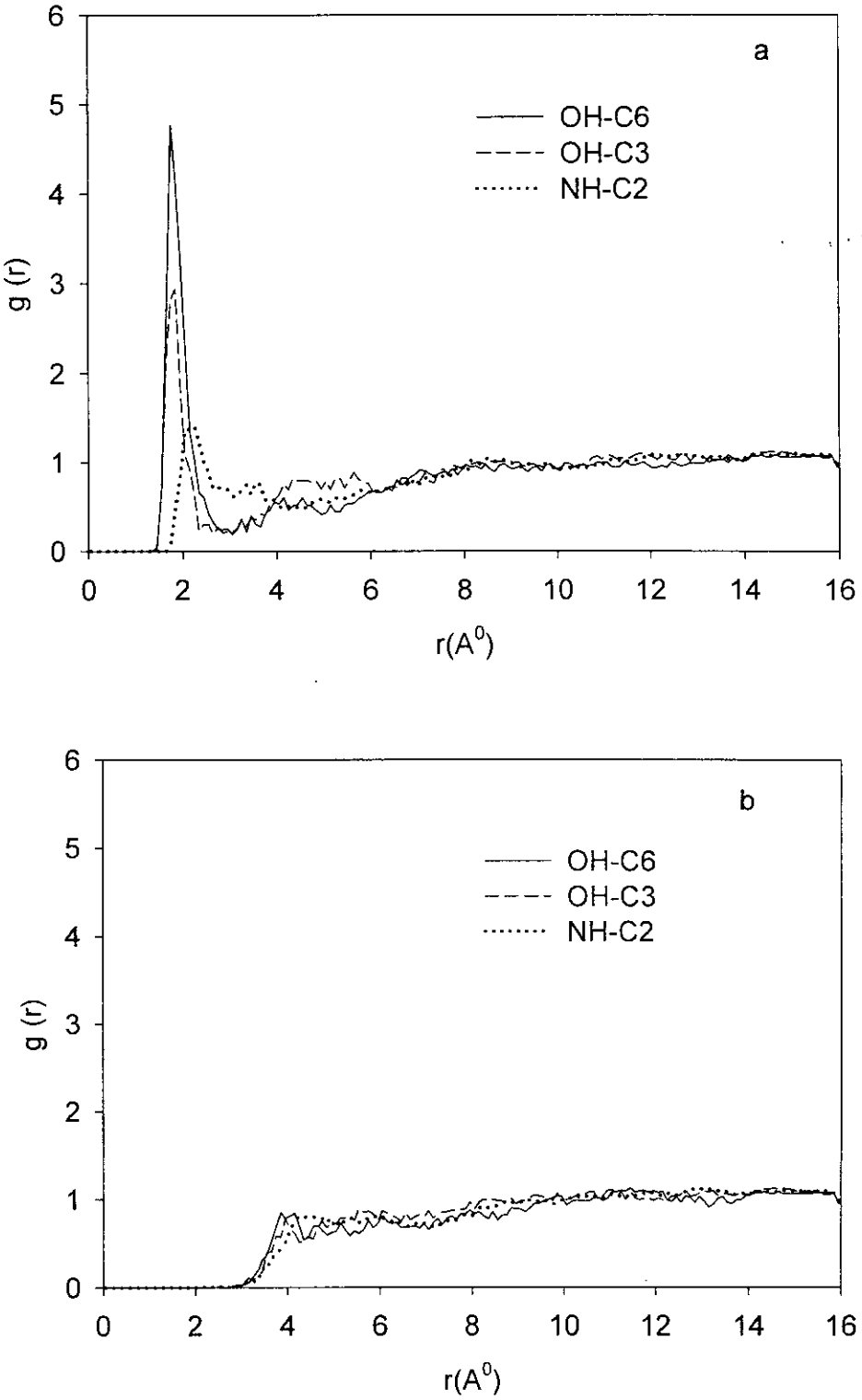

Figure 27 Radial distribution functions for the 50:50 PVP-chitosan blend representing hydrogen atom of OH-C3, OH-C6 and NH-C2 of chitosan relative to the distance of a) the oxygen atom of C=O of PVP and b) the nitrogen atom of PVP.

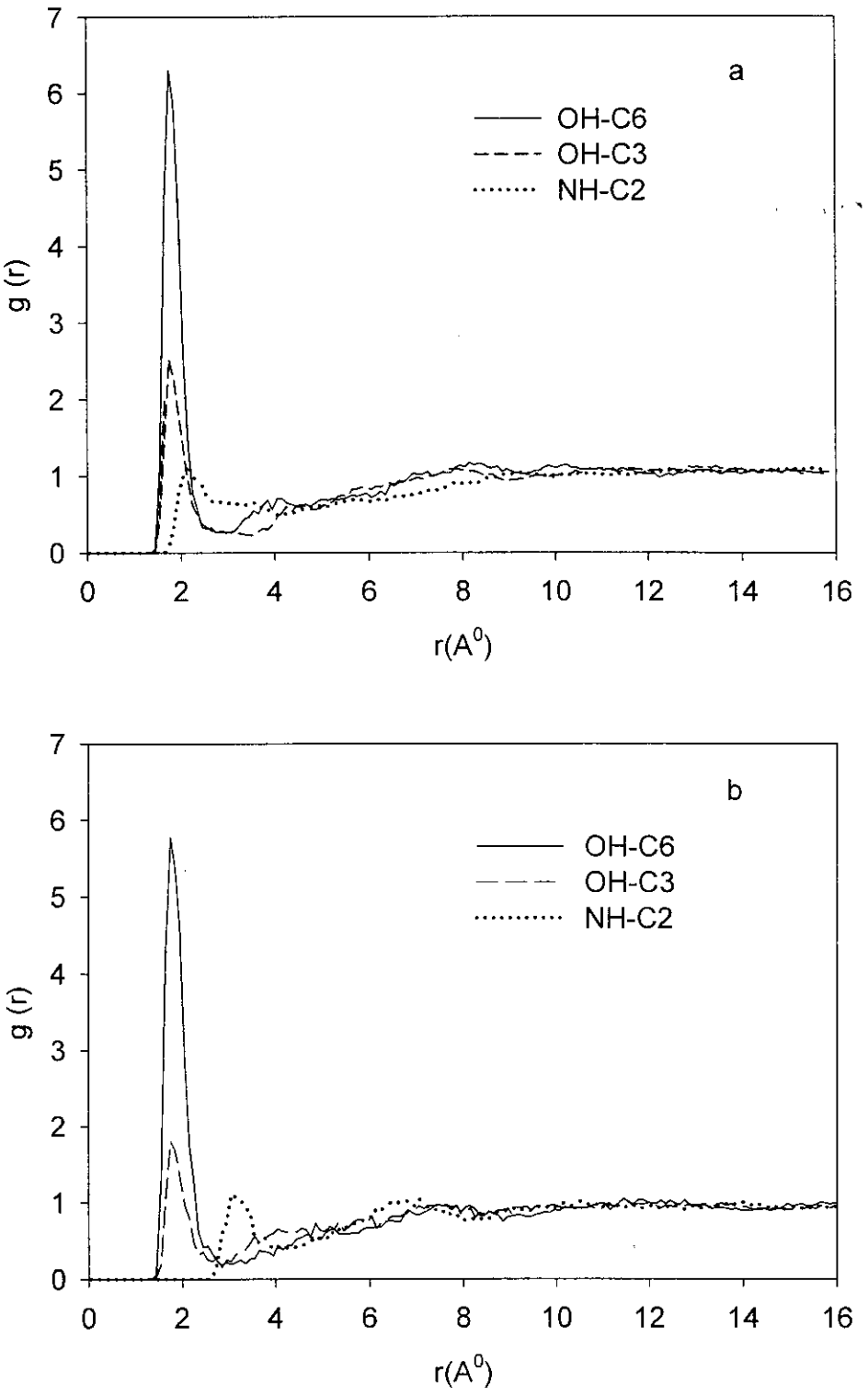

Figure 28 Radial distribution functions for a) 33:67 and b) 20:80 PVP-chitosan blend representing hydrogen atom of OH-C3, OH-C6 and NH-C2 of chitosan relative to the distance of the oxygen atom of C=O of PVP.

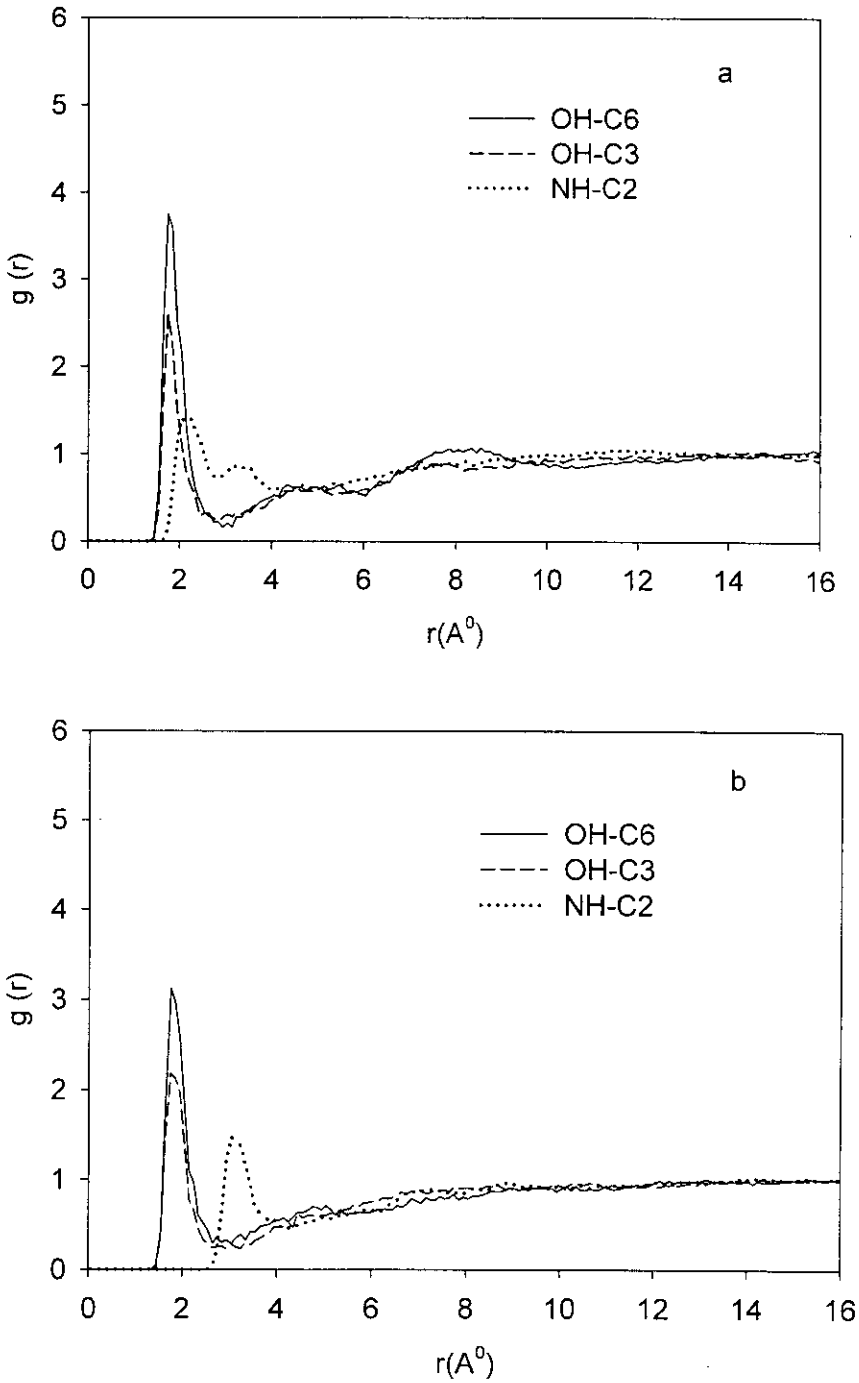

Figure 29 Radial distribution functions for a) 67:33 and b) 80:20 PVP-chitosan blend representing hydrogen atom of OH-C3, OH-C6 and NH-C2 of chitosan relative to the distance of the oxygen atom of C=O of PVP.

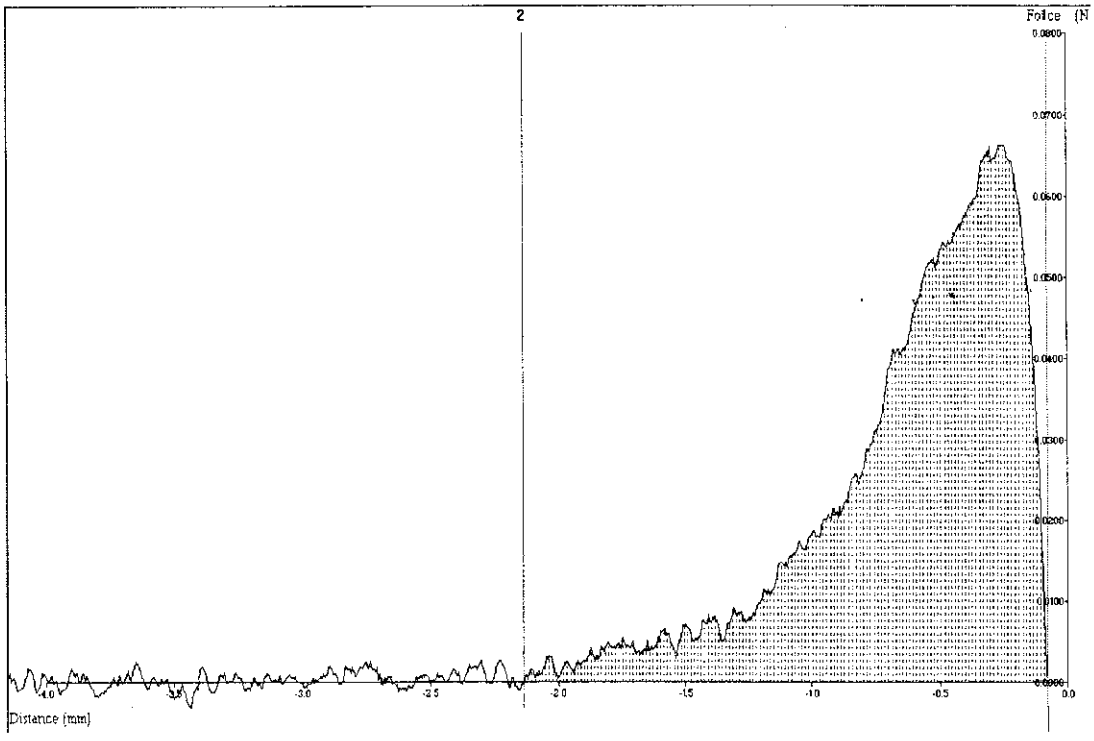

Figure 30 Plot of force VS distance curve (work of adhesion) for chitosan-poly(vinyl pyrrolidone) blend from texture analyzer

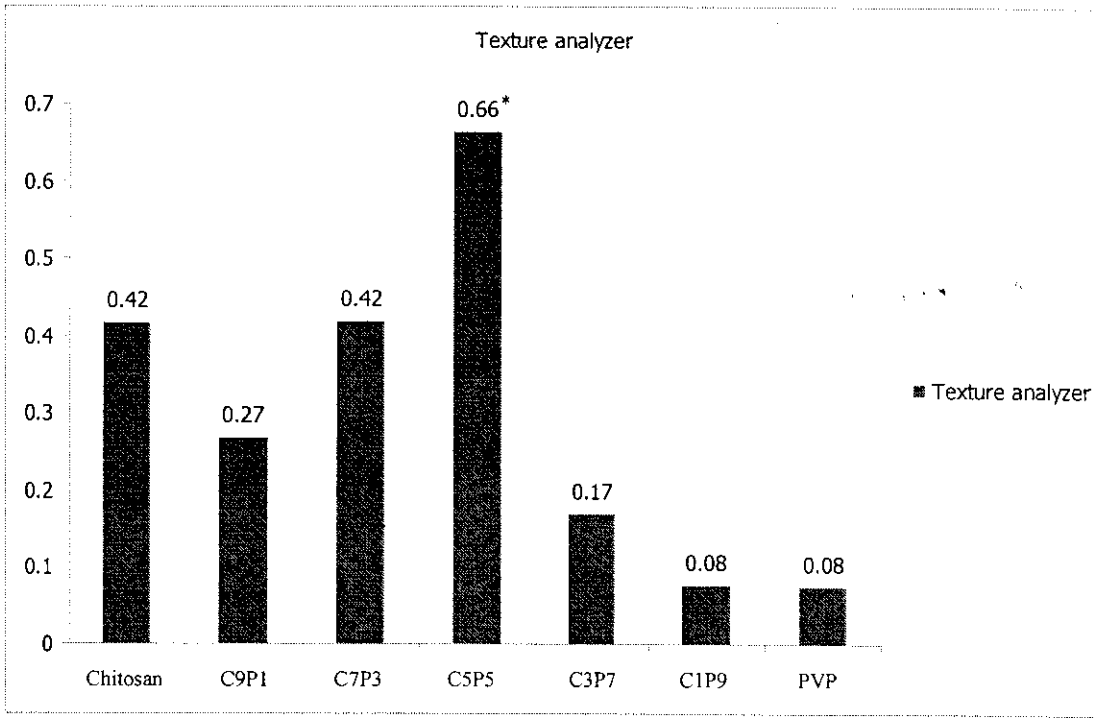

Figure 31 Work of adhesion values of chitosan (C)-poly(vinyl pyrrolidone) (P) blends ratios of 1:9 (C1P9), 3:7 (C3P7), 5:5 (C5P5), 7:3 (C7P3) and 9:1 (C9P1).

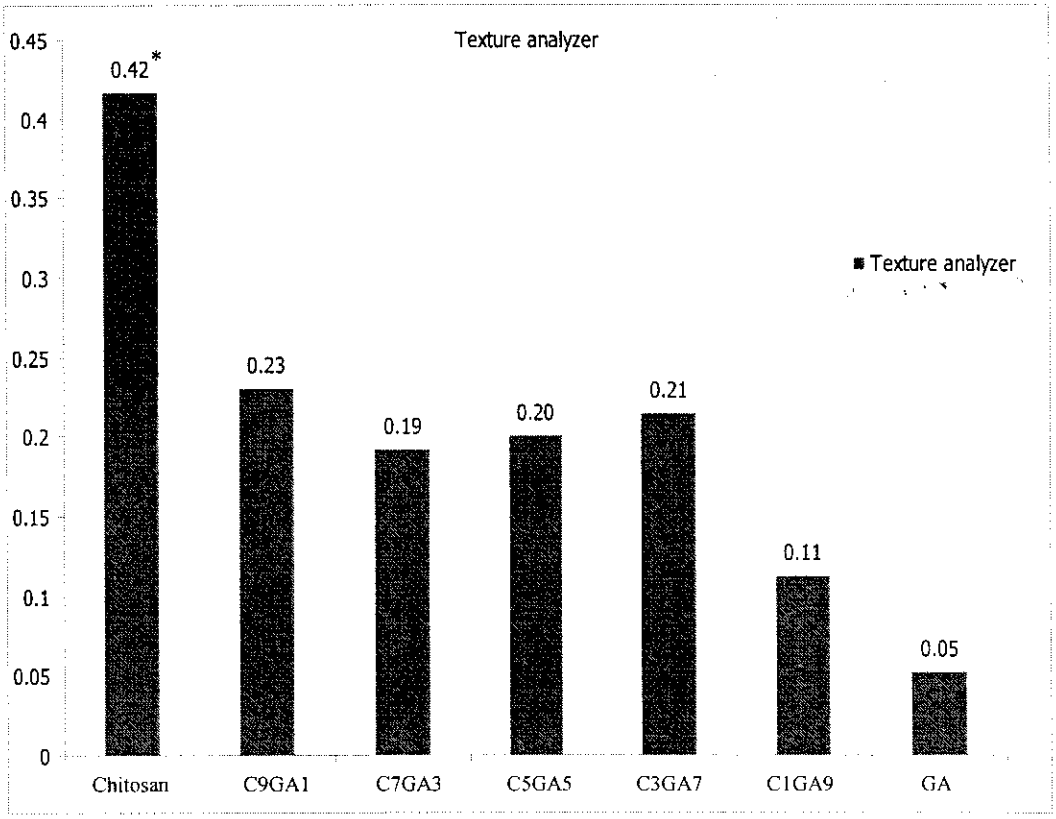

Figure 32 Work of adhesion values of chitosan (C)-gelatin A (GA) blends ratios of 1:9 (C1GA9), 3:7 (C3GA7), 5:5 (C5GA5), 7:3 (C7GA3) and 9:1 (C9GA1).

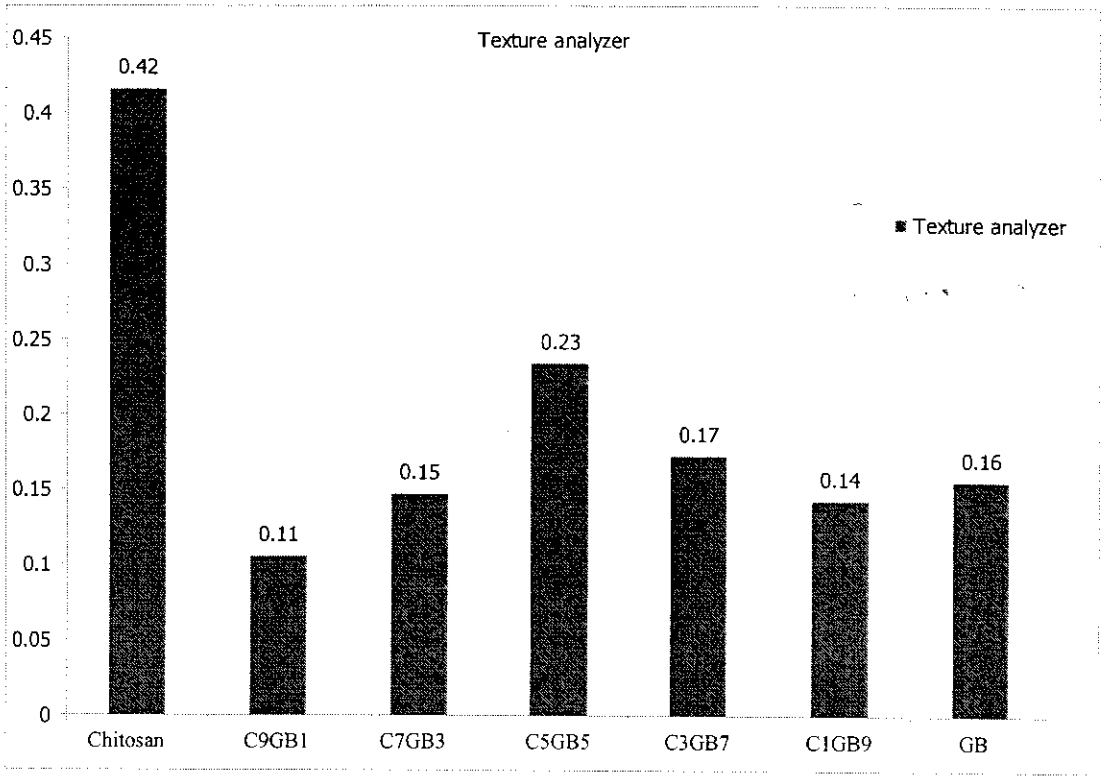

Figure 33 Work of adhesion values of chitosan (C)-gelatin B (GB) blends ratios of 1:9 (C1GB9), 3:7 (C3GB7), 5:5 (C5GB5), 7:3 (C7GB3) and 9:1 (C9GB1).

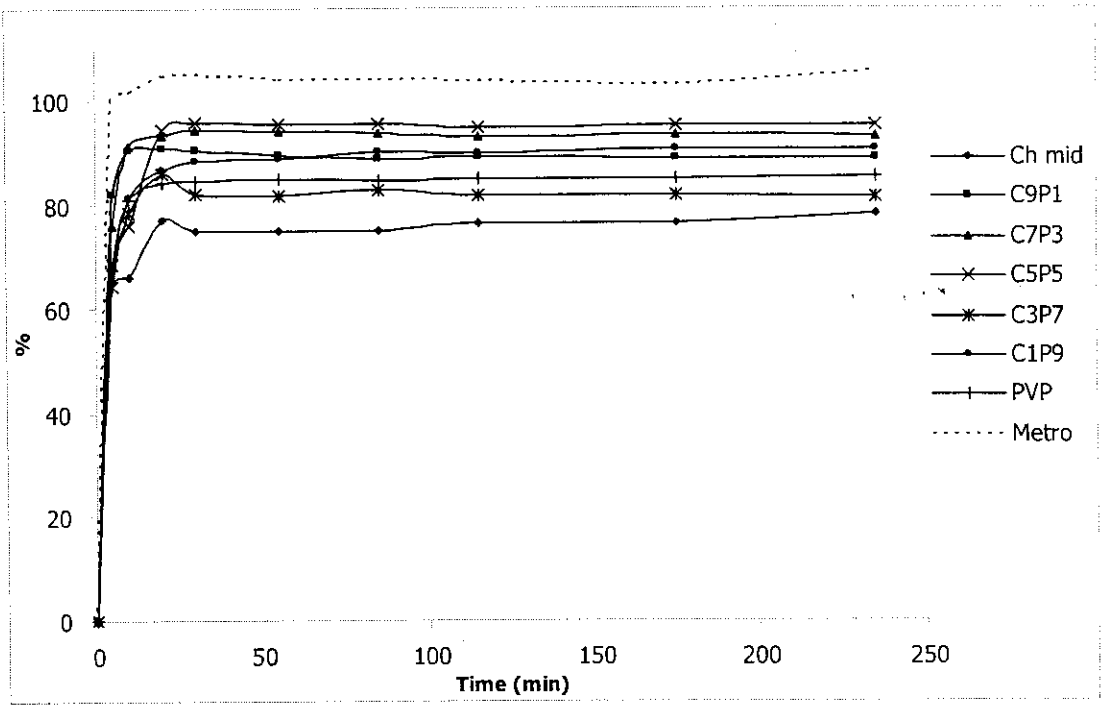

Figure 34 Dissolution profile of metronidazole alone and in various volume ratios of chitosan (C)-poly(vinyl pyrrolidone) (P) blend ratios of 1:9 (C1P9), 3:7 (C3P7), 5:5 (C5P5), 7:3 (C7P3) and 9:1 (C9P1).

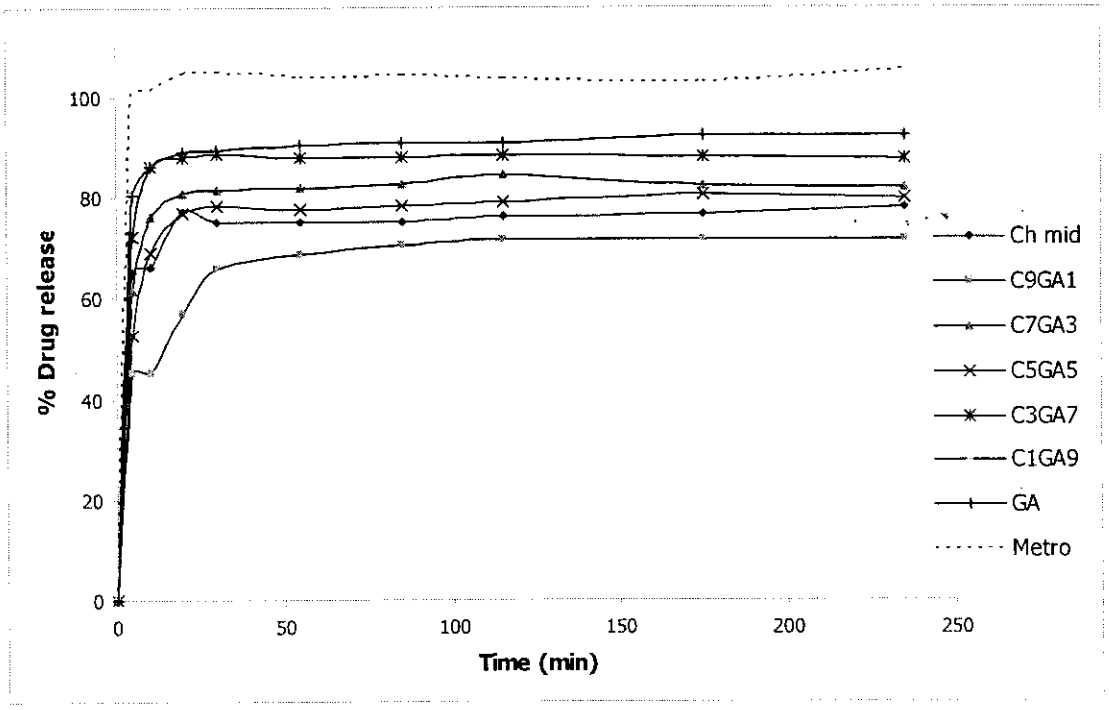

Figure 35 Dissolution profile of metronidazole in various volume ratios of chitosan (C)-gelatin A (GA) blend ratios of 1:9 (C1GA9), 3:7 (C3GA7), 5:5 (C5GA5), 7:3 (C7GA3) and 9:1 (C9GA1).

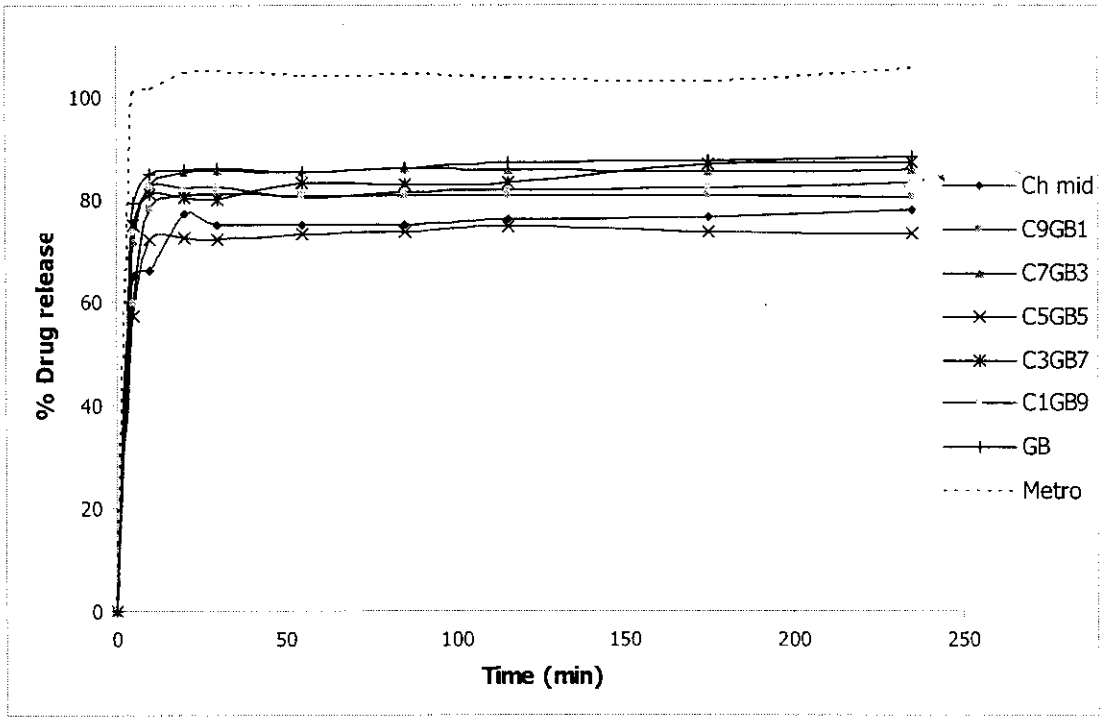

Figure 36 Dissolution profile of metronidazole in various volume ratios of chitosan (C)-gelatin B (GB) blend ratios of 1:9 (C1GB9), 3:7 (C3GB7), 5:5 (C5GB5), 7:3 (C7GB3) and 9:1 (C9GB1).

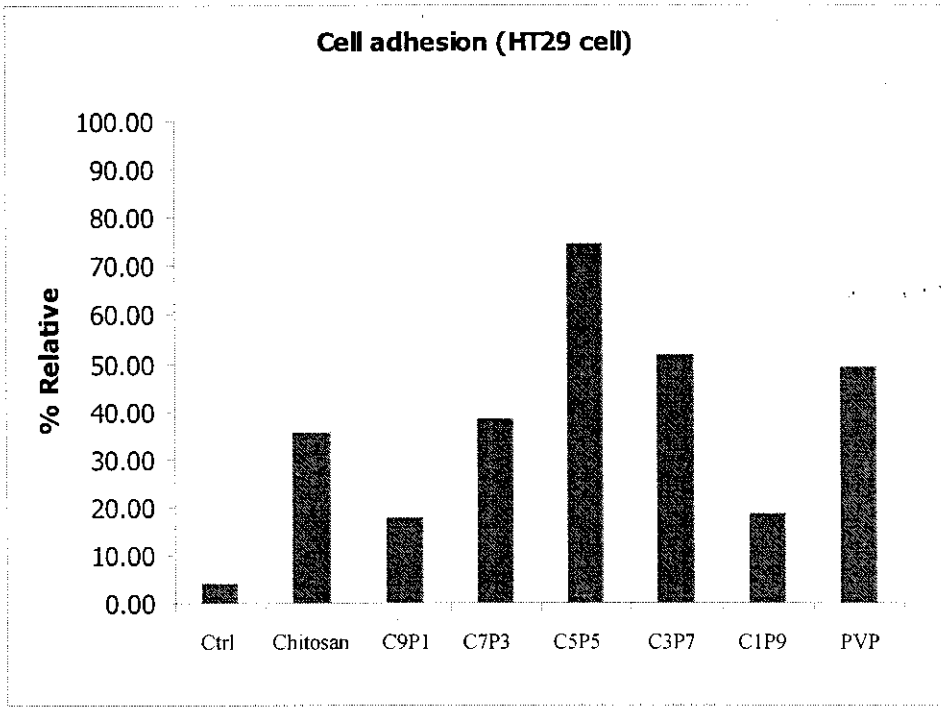

Figure 37 Percent relative HT29 cell attachment of chitosan(C)-PVP ratios of 1:9 (C1P9), 3:7 (C3P7), 5:5 (C5P5), 7:3 (C7P3) and 9:1 (C9P1).

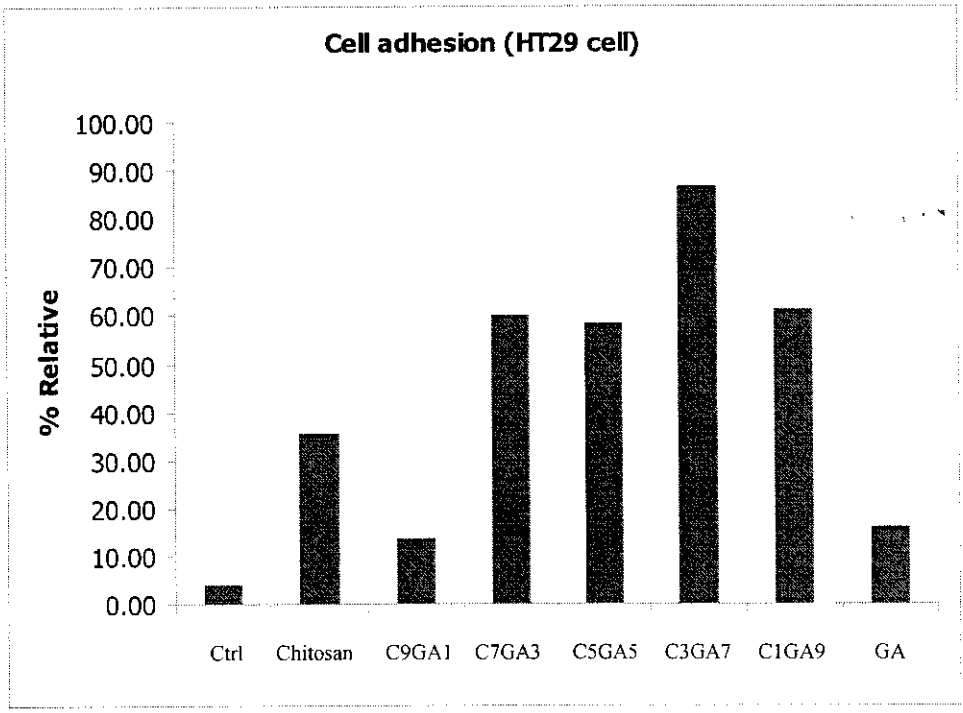

Figure 38 Percent relative HT29 cell attachment of chitosan(C)-gelatin A (GA) ratios of 1:9 (C1GA9), 3:7 (C3GA7), 5:5 (C5GA5), 7:3 (C7GA3) and 9:1 (C9GA1).

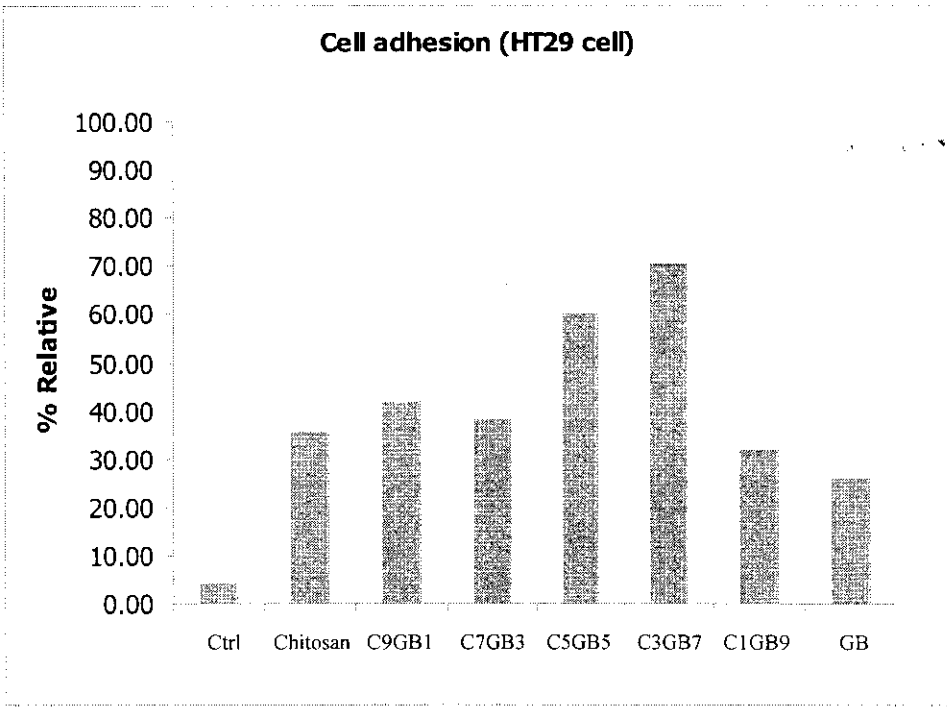

Figure 39 Percent relative HT29 cell attachment of chitosan (C)-gelatin B (GB) ratios of 1:9 (C1GB9), 3:7 (C3GB7), 5:5 (C5GB5), 7:3 (C7GB3) and 9:1 (C9GB1).

Table 1. Polymer (chitosan, polyvinyl pyrrolidone (PVP), blends of chitosan-PVP, and mucin) viscosity (η_p), the component of bioadhesion (η_b), and the force of bioadhesion (F)[1].

Polymer (volume ratio) Chitosan : PVP : Mucin	Final concentration of polymer (%w/v)			η_p	η_b	F
	Chitosan (2.022%)	PVP (2.025%)	Mucin (15.004%)	(cps)	(cps)	(dyne/cm^2)
2.0 : 0.0 : 0.0	0.5055	-	-	14.80 ± 0.10	-	-
2.0 : 0.0 : 5.0	0.5055	-	9.3778	147.00 ± 0.15	14.63 ± 0.15	2.31 ± 0.24
0.0 : 2.0 : 0.0	-	0.5063	-	5.19 ± 0.18	-	-
0.0 : 2.0 : 5.0		0.5063	9.3778	130.58 ± 0.09	7.82 ± 0.09	1.23 ± 0.14
1.8 : 0.2 : 0.0	0.4550	0.0506	-	13.85 ± 0.13	-	-
1.8 : 0.2 : 5.0	0.4550	0.0506	9.3778	145.40 ± 0.05	13.98 ± 0.05	2.21 ± 0.08
1.4 : 0.6 : 0.0	0.3539	0.1518	-	11.55 ± 0.16	-	-
1.4 : 0.6 : 5.0	0.3509	0.1518	9.3778	143.78 ± 0.03	14.66 ± 0.03	2.32 ± 0.04
1.0 : 1.0 : 0.0	0.2528	0.2531	-	9.79 ± 0.10	-	-
1.0 : 1.0 : 5.0	0.2528	0.2531	9.3778	154.82 ± 0.07	27.46 ± 0.07	4.35 ± 0.11
0.6 : 1.4 : 0.0	0.1517	0.3543	-	8.73 ± 0.09	-	-
0.6 : 1.4 : 5.0	0.1517	0.3543	9.3778	151.42 ± 0.19	25.12 ± 0.19	3.98 ± 0.30
0.2 : 1.8 : 0.0	0.0506	0.4556	-	6.62 ± 0.16	-	-
0.2 : 1.8 : 5.0	0.0506	0.4556	9.3778	140.24 ± 0.30	16.06 ± 0.30	2.54 ± 0.48
0.0 : 0.0 : 5.0	-	-	9.3778	117.57 ± 0.05		

[1]Values reported as the mean ± SD (n = 3)

Table 2. Polymer (chitosan, gelatin A, blends of chitosan-gelatin A, and mucin) viscosity (η_p), the component of bioadhesion (η_b), and the force of bioadhesion (F)[1].

Polymer (volume ratio) Chitosan : Gelatin A : Mucin	Final concentration of polymer (%w/v)			η_p	η_b	F
	Chitosan (2.002%)	Gelatin A (2.018%)	Mucin (15.040%)	(cps)	(cps)	(dyne/cm^2)
2.0 : 0.0 : 0.0	0.5005	-	-	13.15 ± 0.02	-	-
2.0 : 0.0 : 5.0	0.5005	-	9.4000	128.33 ± 0.07	16.28 ± 0.07	2.58 ± 0.10
0.0 : 2.0 : 0.0	-	0.5044	-	16.71 ± 0.10	-	-
0.0 : 2.0 : 5.0		0.5044	9.4000	116.71 ± 0.05	1.10 ± 0.05	0.17 ± 0.08
1.8 : 0.2 : 0.0	0.4505	0.0504	-	11.62 ± 0.05	-	-
1.8 : 0.2 : 5.0	0.4505	0.0504	9.4000	124.81 ± 0.04	14.29 ± 0.04	2.26 ± 0.06
1.4 : 0.6 : 0.0	0.3504	0.1513	-	10.66 ± 0.27	-	-
1.4 : 0.6 : 5.0	0.3504	0.1513	9.4000	116.80 ± 0.02	7.24 ± 0.02	1.14 ± 0.04
1.0 : 1.0 : 0.0	0.2503	0.2522	-	9.73 ± 0.04	-	-
1.0 : 1.0 : 5.0	0.2503	0.2522	9.4000	117.37 ± 0.05	8.74 ± 0.05	1.35 ± 0.08
0.6 : 1.4 : 0.0	0.1502	0.3531	-	7.73 ± 0.04	-	-
0.6 : 1.4 : 5.0	0.1502	0.3531	9.4000	113.90 ± 0.17	7.27 ± 0.04	1.15 ± 0.28
0.2 : 1.8 : 0.0	0.0501	0.4539	-	7.91 ± 0.17	-	-
0.2 : 1.8 : 5.0	0.0501	0.4539	9.4000	109.20 ± 0.09	2.39 ± 0.09	0.38 ± 0.14
0.0 : 0.0 : 5.0	-	-	9.4000	98.90 ± 0.25		

[1]Values reported as the mean ± SD (n = 3)

Table 3. Polymer (chitosan, gelatin B, blends of chitosan-gelatin B, and mucin) viscosity (η_p), the component of bioadhesion (η_b), and the force of bioadhesion (F)[1].

Polymer (volume ratio) Chitosan : Gelatin : B/Mucin	Final concentration of polymer (%w/v)			η_p	η_b	F
	Chitosan (2.014%)	Gelatin B (2.042%)	Mucin (15.069%)	(cps)	(cps)	(dyne/cm^2)
2.0 : 0.0 : 0.0	0.5035	-	-	16.12 ± 0.01	-	-
2.0 : 0.0 : 5.0	0.5035	-	9.4181	133.23 ± 0.09	15.54 ± 0.09	2.46 ± 0.15
0.0 : 2.0 : 0.0	-	0.5105	-	7.48 ± 1.98	-	-
0.0 : 2.0 : 5.0	-	0.5105	9.4181	112.65 ± 0.11	3.59 ± 0.11	0.57 ± 0.18
1.8 : 0.2 : 0.0	0.4532	0.0510	-	14.10 ± 0.03	-	-
1.8 : 0.2 : 5.0	0.4532	0.0510	9.4181	126.67 ± 0.07	10.99 ± 0.07	1.74 ± 0.11
1.4 : 0.6 : 0.0	0.3525	0.1532	-	11.00 ± 0.14	-	-
1.4 : 0.6 : 5.0	0.3525	0.1532	9.4181	125.02 ± 0.65	12.44 ± 0.65	1.97 ± 1.03
1.0 : 1.0 : 0.0	0.2518	0.2553	-	9.05 ± 0.13	-	-
1.0 : 1.0 : 5.0	0.2518	0.2553	9.4181	132.67 ± 0.14	22.04 ± 0.14	3.49 ± 0.23
0.6 : 1.4 : 0.0	0.1511	0.3574	-	7.63 ± 0.08	-	-
0.6 : 1.4 : 5.0	0.1511	0.3574	9.4181	133.14 ± 0.09	23.94 ± 0.09	3.79 ± 0.15
0.2 : 1.8 : 0.0	0.0504	0.4595	-	6.67 ± 0.09	-	-
0.2 : 1.8 : 5.0	0.0504	0.4595	9.4181	117.83 ± 0.07	9.58 ± 0.07	1.52 ± 0.10
0.0 : 0.0 : 5.0	-	-	9.4181	101.58 ± 0.11		

[1]Values reported as the mean ± SD (n = 3)

Molecular Modeling Simulation and Experimental Measurements to Characterize Chitosan and Poly(vinyl pyrrolidone) Blend Interactions

KRIT SUKNUNTHA,[1] VIMON TANTISHAIYAKUL,[1] VISIT VAO-SOONGNERN,[2] YOUSSEF ESPIDEL,[3] TERRENCE COSGROVE[3]

[1]Department of Pharmaceutical Chemistry, Faculty of Pharmaceutical Sciences, Prince of Songkla University, Hat-Yai, Songkhla 90112, Thailand

[2]School of Chemistry, Institute of Science, Suranaree University of Technology, Nakhon Ratchasima 30000, Thailand

[3]School of Chemistry, University of Bristol, Cantock's Close, Bristol BS8 1TS, United Kingdom

Received 6 November 2007; accepted 18 March 2008
DOI: 10.1002/polb.21460
Published online in Wiley InterScience (www.interscience.wiley.com).

ABSTRACT: Blends of chitosan and poly(vinyl pyrrolidone) (PVP) have a high potential for use in various biomedical applications and in advanced drug-delivery systems. Recently, the physical and chemical properties of these blends have been extensively characterized. However, the molecular interaction between these two polymers is not fully understood. In this study, the intermolecular interaction between chitosan and PVP was experimentally investigated using ^{13}C cross-polarization magic angle-spinning nuclear magnetic resonance (^{13}C CP/MAS NMR) and diffuse reflectance infrared Fourier transform spectroscopy (DRIFTS). According to these experimental results, the interaction between the polymers takes place through the carbonyl group of PVP and either the OH—C_6, OH—C_3, or NH—C_2 of chitosan. In an attempt to identify the interacting groups of these polymers, molecular modeling simulation was performed. Molecular simulation was able to clarify that the hydrogen atom of OH—C_6 of chitosan was the most favorable site to form hydrogen bonding with the oxygen atom of C=O of PVP, followed by that of OH—C_3, whereas that of NH—C_2 was the weakest proton donor group. The nitrogen atom of PVP was not involved in the intermolecular interaction between these polymers. Furthermore, the interactions between these polymers are higher when PVP concentrations are lower, and interactions decrease with increasing amounts of PVP. © 2008 Wiley Periodicals, Inc. J Polym Sci Part B: Polym Phys 46: 1258–1264, 2008
Keywords: chitosan; ^{13}C CP/MAS NMR; DRIFTS; molecular dynamics; poly(vinyl pyrrolidone)

INTRODUCTION

Polymer blends have received a great deal of attention in the recent years, because blending is a simple and effective method to develop new materials with specific properties that cannot be achieved by the individual polymer. Chitosan, (1-4)-2-amino-2-deoxy-β-D-glucan, is a natural polymer obtained by alkaline deacetylation of chitin, (1-4)-2-acetamido-2-deoxy-β-D-glucan. The molecule contains amino and hydroxyl groups on its backbone, which can serve as proton donors/proton acceptors in hydrogen-bonding interaction between chitosan molecules or

Correspondence to: V. Tantishaiyakul (E-mail: vimon.t@psu.ac.th)
Journal of Polymer Science: Part B: Polymer Physics, Vol. 46, 1258–1264 (2008)

between chitosan and other polymers. Chitosan has been widely investigated for its potential use in industrial, medical, and pharmaceutical applications. In addition to the use of chitosan as a single polymer, it is also often blended with various other hydrophilic polymers.[1,2] Chitosan and poly(vinyl pyrrolidone) (PVP) blends have been prepared and investigated for their potential use as controlled release drug-delivery systems, and for enhancing mucoadhesive properties.[3,4] Both chitosan and PVP (Fig. 1) are biocompatible and nontoxic, and they demonstrate interesting biological properties.[5–7]

Generally, the important factor that determines the properties of a blend is the compatibility/miscibility of polymer pairs. The chemical structures of the polymeric components have a significant effect on the interactions between the polymers resulting in miscibility of the polymer blend. For chitosan and PVP blends, both the hydroxyl and the amine functional groups of chitosan have the potential to interact with the amide groups of PVP via hydrogen bonding. Various methods including viscosity measurement,[7–9] differential scanning calorimetry (DSC),[10] and Fourier transform infrared (FTIR) spectroscopy[8] have been previously used to explore the interactions between these two polymers. Nevertheless, most of these experimental studies have not been able to reveal which of the two hydroxyl groups (i.e., at C_6 and at C_3) and/or amine group at C_2 of chitosan are involved in the interaction in these blends.

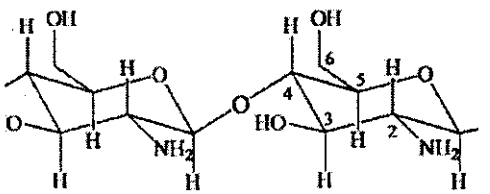

Chitosan

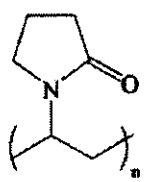

Poly(vinyl pyrrolidone)

Figure 1. Structures of chitosan and poly(vinyl pyrrolidone).

Molecular modeling has been effectively used to study the interaction between two different species based on the calculation of radial distribution function (RDF).[11,12] In this study, molecular dynamics simulations and RDF calculations have been performed with the aim to deduce the specific groups of chitosan that are responsible for intermolecular interaction with PVP. In addition to this computational method, the interactions between these two polymers have also been evaluated using ^{13}C solid-state nuclear magnetic resonance (NMR) and diffuse reflectance infrared Fourier transform spectroscopy (DRIFTS).

EXPERIMENTAL

Chitosan, middle viscosity with a degree of deacetylation of 75–85%, was obtained from Fluka. PVP K-90 (Kollidon 90), with an average molecular weight ($\overline{M}_w$) of 1,100,000, was kindly supplied by BASF, Thailand. All other reagents were of analytical grade.

Preparation of the Blend

Chitosan solution was prepared by dissolving 1.5031 g of chitosan in 50 mL (0.05 M) HCl at ambient temperature with constant stirring overnight. PVP (1.5043 g) was dissolved in water purified by reversed osmosis. The PVP solution was mixed with the chitosan solution in a 1:1 volume ratio. The solution of this blend was lyophilized to obtain the solid blend.

DRIFTS Spectra Collection

The samples were placed in a microsample cup for PerkinElmer Spectrum One FTIR diffuse reflectance accessory using the supplied sample cup holder. The FTIR measurements were performed on a PerkinElmer Spectrum One and a PerkinElmer DRIFTS accessory. The spectra were recorded from 4400 to 450 cm^{-1} by averaging 64 scans at 4 cm^{-1} resolution. All reflectance spectra were converted to Kubelka-Munk (KM) unit by the use of PerkinElmer Spectrum for Windows version 5.02 software package.

^{13}C Solid-State NMR

The NMR experiments were performed on a Bruker Avance 300 NMR spectrometer operating at 75.51 MHz for ^{13}C using standard 4 mm cross-polarization magic angle-spinning probes (CP/MAS). The samples were spun at the magic angle at a rate of 10620 Hz with a total number scans of 10,000. A ^{13}C contact time of 5.0 ms was used, and a recycle delay between scans for all the samples was 3 s. The ^{13}C chemical shifts were referenced with respect to tetramethylsilane (=0 ppm) using solid adamantine as a secondary standard. There were no spinning side band (SSB) interferences due to the fact that the samples were spun at 10 kHz. The deconvolution of NMR spectra was performed using GRAMS/AI (7.01) by fitting the spectra with a Gaussian function.

Computational Method

Simulations of chitosan and PVP blend were performed using Materials Studio 4.2 (Accelrys) on a dual core Pentium-based computer. A COMPASS (condensed-phase optimized molecular potentials for atomistic simulation studies) force field was used for all calculations. This force field has been widely used to optimize and predict the conformation and thermophysical condensed phase properties of a broad range of molecules and polymers.[13]

Polymer assemblies containing three chains of PVP (20 monomer units) in its atatic stereochemical structure and three chains of chitosan (10 monomer units) were generated for the simulation of a 50/50 composition of the blend as previously conducted.[14] For the simulation of PVP/chitosan 20/80, 33/67, 67/33, and 80/20 blends, three chains of each polymer were also used, but the numbers of monomer units were 20/40, 20/20, 40/10, and 80/10, respectively. Each generated polymer chain was minimized using the Discover module, and the blend systems were built inside a box with periodic boundary conditions constructed using the amorphous cell module of the Materials Studio. The density of the blend system was estimated from densities of the pure polymers, that is, 1.04 g/cm^3 for PVP and 0.67 g/cm^3 for chitosan.[14] Thus, the simulation cell densities for PVP/chitosan 20/80, 33/67, 50/50, 67/33, and 80/20 were 0.744, 0.792, 0.855, 0.917, and 0.966 g/cm^3, respectively. The polymer assemblies were energy minimized using the steepest descent method followed by the conjugate gradient method with a convergence level of 0.01 kcal/mol/Å. Group-based cutoff of 12.5 Å and a switching function with the spline and buffer widths of 3 and 1 Å, respectively, were applied to evaluate nonbonded interactions. Molecular dynamics simulations were performed in the NVT ensemble (constant particle numbers, volume, and temperature) at 298 K with a time step of 1 fs. Molecular dynamics simulations were run for 1500 ps. Subsequently, the calculation of RDF, $g(r)$, was carried out of the trajectory files of simulations where the dynamic shows a stable performance.

RESULTS AND DISCUSSION

The ^{13}C NMR chemical shifts or line shapes of carbon resonance in the CP/MAS spectra can provide information about the chemical environment of the carbon nucleus; therefore, their changes can indicate the intermolecular interactions between the blend components. The ^{13}C CP/MAS NMR spectra of PVP, chitosan, and the 50/50 PVP/chitosan blend are shown in Figure 2. According to these ^{13}C CP/MAS NMR spectra, the chemical shift of the PVP carbonyl carbon is observed at 176.23 ppm. This carbonyl carbon peak of the blend appears almost in the same chemical shift. However, its shape is broader and asymmetric compared to that of the pure PVP. Chen et al.[15] have resolved ^{13}C CP/MAS NMR spectra at the carbonyl region to identify

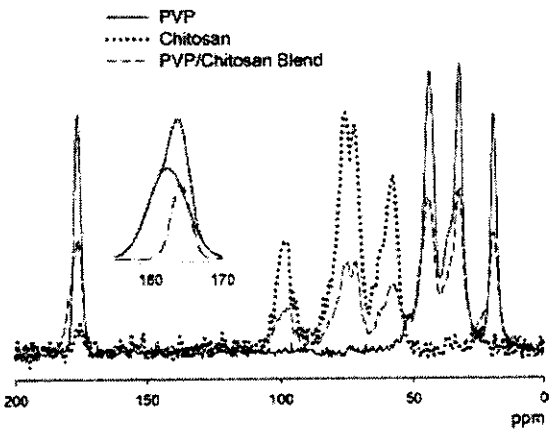

Figure 2. ^{13}C CP/MAS NMR spectra of chitosan, PVP and 50/50 PVP/chitosan blend; inset: the resolved spectrum of C=O band of the 50/50 PVP/chitosan blend.

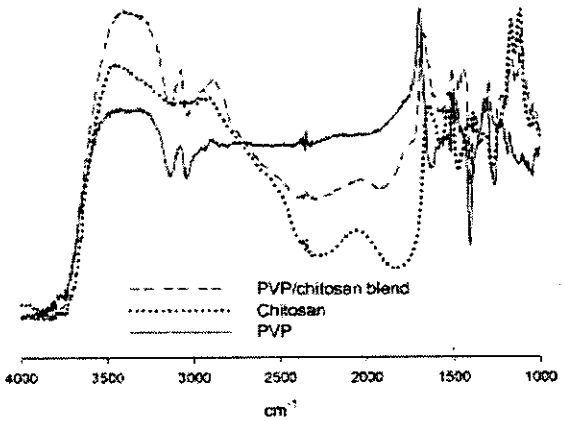

Figure 3. DRIFTS spectra of chitosan, PVP, and 50/50 PVP/chitosan blend.

the crystalline and amorphous fractions of materials. In this study, the carbonyl carbon peak of PVP in the blend was resolved into two Gaussian peaks using a curve-fitting procedure (inset, Fig. 2). PVP is an amorphous material. According to X-ray diffraction result, the PVP/chitosan blend is also amorphous (data not shown). Hence, these two resolved peaks will not specify whether the form of PVP present is amorphous or crystalline. Multipeak curve fitting of NMR spectra has been previously signified as the occurrence of different interactions or environments of a specific group.[16,17] Thus, in this study, the downfield shift of one peak may possibly result from the intermolecular hydrogen bonding between the carbonyl group of PVP and the hydrogen atom of OH—C_6, OH—C_3, or NH—C_2 group of chitosan. The other peak may be the unreacted carbonyl carbon. As shown in Figure 2, the chemical shift of C_2 and C_6 of chitosan appears at 57.65 ppm and that of carbon atom C_3 displays at 71.69 ppm, which correspond to the previous assignment.[18] The upfield shifts of 0.70 (from 57.65 to 56.95 ppm) and 0.39 ppm (from 71.69 to 71.30 ppm) were observed for C_2/C_6 and C_3, respectively, of the blend. As previously observed, the upfield shift of a carbon atom is attributed to the formation of hydrogen bonds of a connected proton donor group.[19] In this study, the upfield shifts may therefore result from the intermolecular bonding between the proton donors of the OH groups at C_3 and/or C_6 as well as the NH group at C_2 with C=O of PVP.

In addition to ^{13}C CP/MAS NMR, DRIFTS was used to investigate the interactions between these two polymers. Figure 3 shows DRIFTS spectra of PVP, chitosan, and the 50/50 PVP/chitosan blend. The spectrum of pure chitosan shows an amino band at 1637 cm^{-1}. In addition, chitosan displays a broad peak at around 3400 cm^{-1}, resulting from the N—H and O—H vibrations. The amide carbonyl stretching of PVP shows a prominent peak at 1685 cm^{-1}. In the blend, this peak is shifted to the lower wavenumber at 1669 cm^{-1} indicating the incidence of interaction between PVP and chitosan. This interaction is attributed to the hydrogen bonds formed between the proton acceptor C=O of the PVP and the proton donor groups, such as OH—C_6, OH—C_3, and NH—C_2 groups, of chitosan. Because of the overlapping band of OH and NH functions of chitosan, it is somewhat difficult to indicate which group is the proton donor in this system.

Molecular dynamics simulations and subsequent RDF calculations were performed to investigate the specific proton donor group of chitosan that interacts with the proton acceptor group of PVP. The RDF, also referred to as pair-correlation function, demonstrates the average density of atoms at a distance from a specified atom. The RDF analyses were performed in the interval of simulations where the simulation shows a stable behavior, that is, from 800 to 1500 ps as illustrated in Figure 4. Figure 5 displays the intermolecular RDFs for the 50/50 PVP/chitosan blend. As shown in Figure 5(a), a pronounced peak at 1.75 Å with the $g(r)$ function of 4.76 corresponds to the hydrogen bonding between the hydrogen atoms of OH—C_6 of chitosan and the oxygen atoms of C=O of PVP. Meanwhile the $g(r)$ function of about 2.81 at 1.75 Å was observed for hydrogen atoms of OH—C_3 chitosan and oxygen atoms of C=O of PVP. This indicates that hydrogen atoms of OH—C_6 form stronger hydrogen bonds with

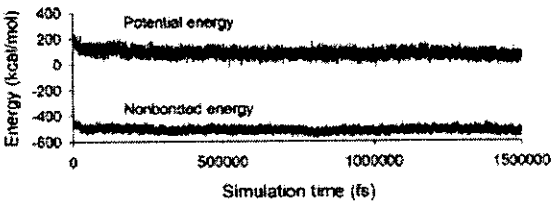

Figure 4. Potential and nonbonded energy vs simulation time of 1500 ps.

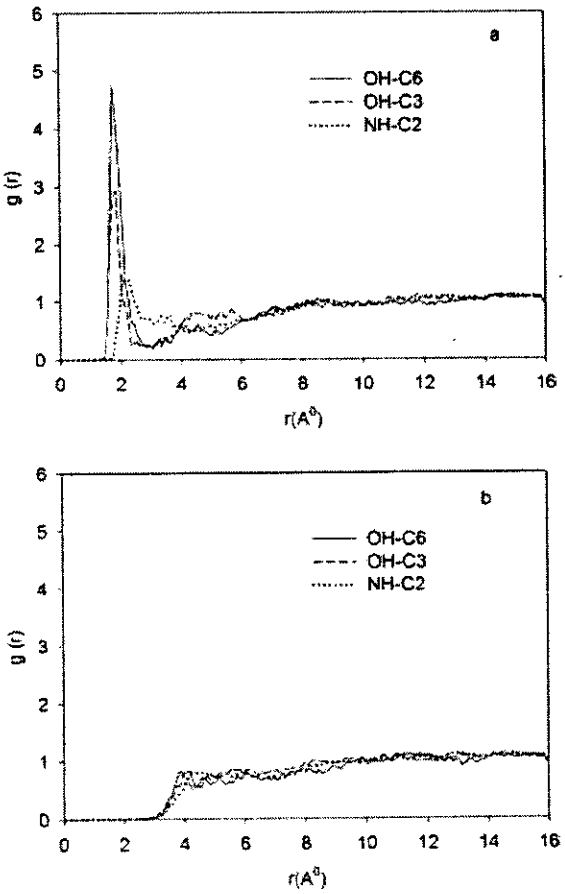

Figure 5. Radial distribution functions for the 50/50 PVP/chitosan blend representing hydrogen atom of OH—C_6, OH—C_3 and NH—C_2 of chitosan relative to the distance of (a) the oxygen atom of C=O of PVP and (b) the nitrogen atom of PVP.

C=O of PVP than hydrogen atoms of OH—C_3. This is possible because of the free rotation of OH—C_6 compared to OH—C_3, and consequently there is more accessibility to interact with oxygen atoms of PVP. This computational model is the first study that distinguishes the proton donor capacity between OH—C_6 and OH—C_3 of chitosan on interacting with other polymers.

The shift of the peak to 2.25 Å with the lower $g(r)$ of 1.41 is related to the hydrogen atoms of NH—C_2 of chitosan and the oxygen atoms of C=O of PVP. Therefore, the intermolecular hydrogen bond involving the amino group as the proton donor is significantly weaker than that of the hydroxyl groups of chitosan. This may be due to the fact that an N—H bond is less polar than an O—H bond. Thus the N—H···O=C hydrogen bond is weaker than the O—H···O=C counterpart. Figure 5(b) displays the RDF calculations for the nitrogen atom of PVP and the proton donors groups of chitosan. It can be observed that the amide nitrogen of PVP is less likely to function as a proton acceptor. Generally, nonbonding electron pairs of the amide nitrogen will delocalize to the carbonyl group. Therefore, in this case, when the proton donors of chitosan interact with the amide function of PVP, they will form a bond at the oxygen atom in preference to the nitrogen atom.

As proton acceptors, the oxygen atoms of the hydroxymethyl groups were previously reported to be more reactive than the nitrogen atoms of the amino groups of chitosan in forming hydrogen bonds with proton donors of polyvinyl alcohol (PVA) or poly(2-hydroxyethyl methacrylate) (P2HEM) at some ratios of these polymer blends.[11,20] However, with the higher amounts of PVA and P2HEM, the interactions with the amino groups of chitosan increase in intensity. Although, in this study, proton donors and acceptors are reversed compared to the above-mentioned investigations, it was of interest to determine the interacting groups at different compositions of our polymer blend. Therefore, molecular dynamic simulations of PVP/chitosan at compositions of 20/80, 33/67, 67/33, and 80/20 were performed, and the RDFs for these blends were presented in Figures 6 and 7. The same results were obtained as the above-mentioned RDF for the 50/50 PVP/chitosan blend, at either lower or higher amounts of PVP, hydrogen atoms of NH—C_2 of chitosan function less as proton donors compared to those of OH—C_6 and OH—C_3. In the previous study, it was also observed that the interactions between hydrogen atoms of NH—C_2 of chitosan and proton acceptor groups of P2HEM at various compositions of these blends were lower than those of the OH groups.[11]

Additionally, at lower amounts of PVP, the $g(r)$ functions observed for the oxygen atom of C=O of PVP and the hydrogen atoms of OH—C_6 and OH—C_3 of chitosan are 6.29 and 2.52, respectively, for the 33/67 PVP/chitosan blend [Fig. 6(a)], and those of 5.76 and 1.70, respectively, for the 20/80 PVP/chitosan blend [Fig. 6(b)]. Furthermore, for higher proportions of PVP, the $g(r)$ functions for the oxygen atom of C=O of PVP and the hydrogen atoms of OH—C_6 and OH—C_3 of chitosan are 3.75 and 2.58, respectively, for the 67/33 PVP/chitosan

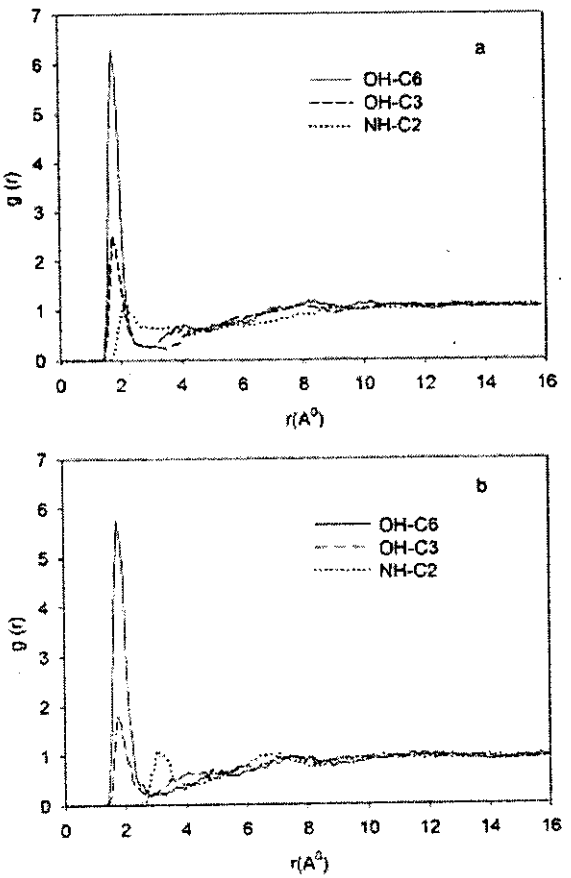

Figure 6. Radial distribution functions for (a) 33/67 and (b) 20/80 PVP/chitosan blend representing hydrogen atom of OH—C_6, OH—C_3 and NH—C_2 of chitosan relative to the distance of the oxygen atom of C=O of PVP.

blend [Fig. 7(a)] and those of 3.12 and 2.17, respectively, for the 80/20 PVP/chitosan blend [Fig. 7(b)]. This indicates that the intermolecular hydrogen bonding between these two polymers is higher with lower amounts of PVP in the blends, and lower with the higher proportions of PVP (Figs. 6 and 7, respectively). According to the previous investigations[4,8] of various compositions of these two polymers blends, it demonstrates that these blends are miscible with only one glass transition temperature (T_g) was detected for each blend. In addition, the DSC thermograms of PVP/chitosan blends from both studies show positive deviations of T_gs from the linearity in the blends with lower PVP proportions whereas T_gs are lower in the blends with high amounts of PVP. Generally, the T_gs of polymer blends will be in the linear line, which ranges between the initial T_g of each polymer depending on the relative amount of each polymer in the blend. However, if the two polymers bind more strongly to each other than to themselves, the T_g will be higher than expected (positive deviation from linearity). If the two polymers bind less strongly with each other than with themselves, the T_gs of the blends are lower than expected (negative deviation). Our dynamic simulations results are consistent with these findings[4,8] in terms of positive/negative deviations related to the forces of intermolecular interactions between the polymers at lower/higher compositions of the PVP.

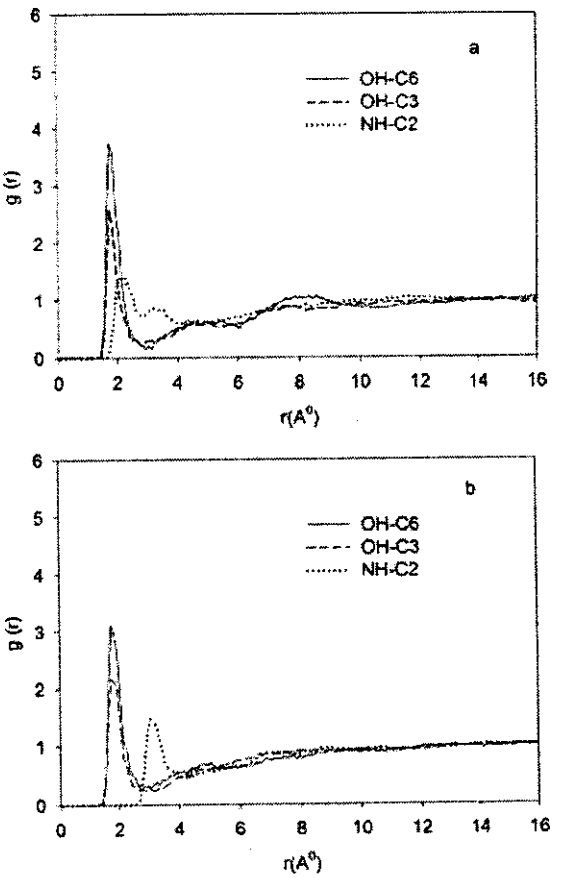

Figure 7. Radial distribution functions for (a) 67/33 and (b) 80/20 PVP/chitosan blend representing hydrogen atom of OH—C_6, OH—C_3 and NH—C_2 of chitosan relative to the distance of the oxygen atom of C=O of PVP.

CONCLUSIONS

^{13}C CP/MAS NMR and DRIFTS spectra demonstrate that the C=O group of PVP interacts with chitosan in the blending of these two polymers. Considering the chemical structures of these molecules, the hydrogen atoms of $OH—C_6$, $OH—C_3$, and $NH—C_2$ of chitosan can possibly function as proton donors in these intermolecular hydrogen-bonding interactions between PVP and chitosan. However, these experimental results have not been able to identify with certainty the specific groups of proton donors. Molecular modeling simulation was then used to identify the proton donor group of chitosan. The computational results are consistent with the experimental findings that intermolecular interactions take place via the C=O of PVP. Additionally, the molecular simulations verify that the hydroxyl groups of chitosan are the more favorable sites for hydrogen-bond formations than the $NH—C_2$ group. The hydrogen atom of $OH—C_3$ is less favorable than that of $OH—C_6$ as a proton donor group. Besides the oxygen atom of PVP, the nitrogen atom is another possible proton acceptor site. According to the computational modeling results, however, this nitrogen atom does not serve as a proton acceptor in these systems. Furthermore, the computational results agree with the previous studies in relating the force of interaction between the polymers to the compositions of the polymers, that is, there is higher interactions with the lower amounts of PVP in the blend and lower interactions with the increasing amounts of PVP in the blend.

This work was supported by the Thailand Research Fund through the Royal Golden Jubilee Ph.D. Program (PHD/0170/2547) to KS, Prince of Songkla University through Grant No. PHA50162, Ministry of Education through the Tailor-made Medicine for the Enhancement of Thailand Competitiveness Project, and the National Nanotechnology Center (NANOTEC), National Science and Technology Development Agency (NSTDA), Ministry of Science and Technology through its National Nanoscience Consortium (CNC).

REFERENCES AND NOTES

1. Khoo, C. G. L.; Frantzich, S.; Rosinski, A.; Sjostrom, M.; Hoogstraate, J. Eur J Pharm Biopharm 2003, 55, 47–56.
2. Lu, L.; Peng, F.; Jiang, Z.; Wang, J. J Appl Polym Sci 2006, 101, 167–173.
3. Patel, V. M.; Prajapati, B. G.; Patel, M. M. Acta Pharm 2007, 57, 61–72.
4. Karavas, E.; Georgarakis, E.; Bikiaris, D. J Therm Anal Cal 2006, 84, 125–133.
5. Brunius, C. F.; Edlund, U.; Albertsson, A. C. J Polym Sci Polym Chem 2002, 40, 3652–3661.
6. Liu, X. F.; Guan, Y. L.; Yang, D. Z.; Li, Z.; Yao, K. D. J Appl Polym Sci 2001, 79, 1324–1335.
7. Abou-Aiad, T. H. M.; Abd-El-Nour, K. N.; Hakim, I. K.; Elsabee, M. Z. Polymer 2006, 47, 379–389.
8. Marsano, E.; Vicini, S.; Skopinska, J.; Wisniewski, M.; Sionkowska, A. Macromol Symp 2004, 218, 251–260.
9. Yilmaz, E.; Ozalp, D.; Yilmaz, O. Int J Polym Anal Charact 2005, 10, 329–339.
10. Sakurai, K.; Maegawa, T.; Takahashi, T. Polymer 2000, 41, 7051–7056.
11. Sandoval, C.; Castro, C.; Gargallo, L.; Radic, D.; Freire, J. Polymer 2005, 46, 10437–10442.
12. Pandit, S. A.; Bostick, D.; Berkowitz, M. L. Biophys J 2003, 84, 3743–3750.
13. Sun, H. J Phys Chem B 1998, 102, 7338–7364.
14. Prathab, B.; Aminabhavi, T. M. Langmuir 2007, 23, 5439–5444.
15. Chen, C.; Dong, L.; Cheung, M. K. Eur Polym J 2005, 41, 958–966.
16. Xu, W.; Luo, Q.; Wang, H.; Francesconi, L. C.; Stark, R. E.; Akins, D. L. J Phys Chem B 2003, 107, 497–501.
17. Miller, J. M.; Lakshmi, L. J. J Phys Chem B 1998, 102, 6465–6470.
18. Heux, L.; Brugnerotto, J.; Desbrieres, J.; Versali, M. F.; Rinaudo, M. Biomacromolecules 2000, 1, 746–751.
19. Miyoshi, T.; Takegoshi, K.; Hikichi, K. Polymer 1997, 38, 2315–2320.
20. Jawalkar, S. S.; Raju, K. V. S. N.; Halligudi, S. B.; Sairam, M.; Aminabhavi, T. M. J Phys Chem B 2007, 111, 2431–2439.